

# EXPLORING SEISMIC DATA INTERPOLATION USING RADIAL BASIS FUNCTION\*

D. Olawoyin-Yussuf<sup>1</sup>, H. Tella<sup>2</sup>

King Fahd University of Petroleum and Minerals, Dharan, Saudi Arabia.

Email:<sup>1</sup> g202110610@kfupm.edu.sa,

<sup>2</sup> g202101450@kfupm.edu.sa

## ABSTRACT

Due to the hindrance posed by field acquisition conditions using reflection seismology method, most seismic data collected may be lacking some traces. These missing traces cause problems in processing and deteriorate the quality of final image. It is pertinent that a data interpolation technique is necessary to give more appealing sub-earth structures. In this report, we used Radial Basis Function (RBF) interpolation techniques (Gaussian, Wendland). In analysing the techniques, Signal-to-Noise-Ratio (SNR), 2D FFT (Wavenumber-frequency) was used in comparison with the normal interpolation k nearest neighbour method. The wendland RBF gave the best result.

**Index Terms**— seismic, interpolation, griddata, RBF, gaussian, wendland

## 1. INTRODUCTION

One of the major problems in signal processing is interpolating missing data during signal analysis. One of a number of applications where filling interpolation is important is seismic data interpolation. Seismic data interpolation is one of the major concerns for the oil and gas company because reflection seismology (a method of determining the sub-earth structure that relies on the generation of artificial seismic waves and the recording of their reflections from different geological layers) does not reveal an accurate image of the sub-earth structure. Traces missing or irregularity which causes low quality of image gathers, severe alias, e.t.c. are ubiquitous in seismic exploration due to ocean currents, drilling platforms, mountains, rivers, and so on making seismic data interpolation pertinent. In this project, we explored radial basis function(RBF) as seismic data interpolation technique.

A plethora of methods have been proposed over the past decade to accurately interpolate missing seismic data. These methods can be categorized into three based on their theories. The first category is based on wave equation principles[1] which obtains good reconstruction in structurally complex situations with the drawback of requiring underlying information. The second category is based on prediction filters[2, 3]

although inhibited by equidistant sampling have the benefit of producing good result without aliasing. Mathematical transforms is the bedrock of the third category. Transforms such as Radon, Sieslet, Curvelet, Fourier although requiring no geological background and having the capacity to fit irregularly or sparsely sampled data have the problem of spectrum leakage. Anti-leakage Fourier Transform[4] was proposed not only to fix the spectrum leakage problem caused by non-uniform Fourier Transform (NUFFT) but also combine the advantages of the three categories mentioned above. RBF as an interpolation technique to fit surface of scattered data[5] providing the best performance for discrete data interpolation making it highly considerable in the field of seismic data interpolation. Four methods of RBF and Anti-leakage Fourier Transform (ALFT) for irregular scattered data[6] was applied reaching a conclusion that Multiquadric (MQ) RBF performs best using the sum of root mean square error (SRMSE) as validation index. Radial basis function interpolation and approximation in k-dimensional space using meshless techniques [7] based on Compactly Supported RBF (CSRBF), the interpolant matrix is sparse making computational complexity lesser with a speed up factor of  $10^4$ . The reduced computational complexity and sparse interpolant matrix made pursuing this interpolation technique for seismic data necessary.

## 2. METHODOLOGY

A function  $f : \mathcal{R}^d \rightarrow \mathcal{R}$  for which its output solely depends on magnitude of its inputs, is referred to as radial e.g.  $f(x) = \phi(\|x\|) = \phi(r)$ , where  $\phi : [0, \infty) \rightarrow \mathcal{R}$  and  $r$  is the length of  $x$  which means that  $\phi$  is constant for input vectors of the same length, we refer to  $\phi$  as radial basis function (RBF)[8]. Let's say we have data consisting of the form  $(x_i, g_i)$  for  $i = 1, 2, \dots, n$ . our desire is to determine an interpolant  $s(x)$ ,  $x \in \mathcal{R}^d$ , which satisfies

$$s(x_i) = g_i, \quad i = 1, 2, \dots, n. \quad (1)$$

\*SUBMITTED FOR EE 562 COURSE PROJECT, NOT TO BE DISTRIBUTED

For an RBF interpolant,  $s(x)$  is required to be a linear combination of translates of  $\phi(x)$ , i.e.

$$s(x) = \sum_{i=1}^n \lambda_i \phi(\|x - x_i\|), x \in \mathcal{R}^d. \quad (2)$$

From (1), it follows that

$$\sum_{i=1}^N \lambda_i \phi(\|x_j - x_i\|) = g_j, j = 1, 2, \dots, M. \quad (3)$$

This can be rewritten in matrix form as

$$\begin{bmatrix} \phi(\|x_1 - x_1\|) & \dots & \phi(\|x_N - x_1\|) \\ \phi(\|x_1 - x_2\|) & \dots & \phi(\|x_N - x_2\|) \\ \vdots & & \vdots \\ \phi(\|x_1 - x_n\|) & \dots & \phi(\|x_N - x_n\|) \end{bmatrix} \begin{bmatrix} \lambda_1 \\ \lambda_2 \\ \vdots \\ \lambda_n \end{bmatrix} = \begin{bmatrix} g_1 \\ g_2 \\ \vdots \\ g_n \end{bmatrix} \quad (4)$$

or

$$A\lambda = g. \quad (5)$$

Where  $N \leq M$ . We want to determine  $\lambda = [\lambda_1, \dots, \lambda_N]^T$  by minimizing a quadratic form[7]

$$\frac{1}{2} \lambda^T \mathbf{Q} \lambda. \quad (6)$$

with linear constraint  $A\lambda - g = 0$ , where  $\mathbf{Q}$  is a positive and symmetric matrix. Solving this with Lagrange multipliers  $\zeta = [\zeta_1, \dots, \zeta_M]^T$ , i.e. minimizing

$$\frac{1}{2} \lambda^T \mathbf{Q} \lambda - \zeta^T (A\lambda - g) \quad (7)$$

Finding optimum  $\lambda$  and  $\zeta$  by partial derivatives, would yield

$$\begin{aligned} \mathbf{Q}\lambda - A^T \zeta &= 0 \\ A^T \lambda - g &= 0 \end{aligned} \quad (8)$$

Rewriting in matrix form as

$$\begin{bmatrix} \mathbf{Q} & -A^T \\ A & 0 \end{bmatrix} \begin{bmatrix} \lambda \\ \zeta \end{bmatrix} = \begin{bmatrix} 0 \\ g \end{bmatrix} \quad (9)$$

As  $\mathbf{Q}$  is positive definite, solving (9) yields

$$\begin{aligned} \lambda &= \mathbf{Q}^{-1} A^T (A \mathbf{Q}^{-1} A^T)^{-1} g, \\ \zeta &= (A \mathbf{Q}^{-1} A^T)^{-1} g. \end{aligned} \quad (10)$$

For the problem of seismic data interpolation, we would mostly be concerned with two variable functions. Say a set of  $N$  irregular spaced input data points in the plane:

$$\mathcal{R}^2 = \{(x_i, y_i) : i = 1, 2, \dots, N\}, \quad (11)$$

where data points  $(x_i, y_i), \dots, (x_N, y_N)$ , are all unique and having values  $Z = \{z_i = g(x_i, y_i) : i = 1, 2, \dots, N\}$ . From (2) we have:

$$g(x, y) = \sum_i^N \lambda_i \phi(\|x - x_i\|, \|y - y_i\|), (x_i, y_i) \in \mathcal{R}^2 \quad (12)$$

where  $\phi(\cdot)$  is the RBF, coefficients  $\{\lambda_i\}$  are real and  $\|\cdot\|$  means euclidean norm defined in n-dimensional space as:

$$\|(x, y) - (x_i, y_i)\| = \sqrt{\sum_{m=1}^n [(x, y)_m - (x_i, y_i)_m]^2}. \quad (13)$$

In general, there are two main categories of RBFs[7]:

1. global e.g. Gaussian
2. local e.g. Compactly Supported RBF (Wendland)

Gaussian RBF can be expressed as

$$\phi(\|(x, y) - (x_i, y_i)\|) = \exp\left(-\frac{\|(x, y) - (x_i, y_i)\|^2}{2\sigma^2}\right). \quad (14)$$

For simplicity, we would define the euclidean norm as  $r$  i.e.  $r = \|(x, y) - (x_i, y_i)\|$ , so (14) can be rewritten as

$$\phi(r) = \exp\left(-\frac{r^2}{2\sigma^2}\right) \quad (15)$$

where  $\sigma$  is the variance.

Truncated power functions (Askey's power functions) given by

$$\phi_\ell = (1 - \|x\|_2)_+^\ell = \begin{cases} (1 - \|x\|_2)^\ell & \text{for } 1 - \|x\|_2 \geq 0; \\ 0 & \text{for } 1 - \|x\|_2 \leq 0, \end{cases} \quad (16)$$

have a contact support in the disk  $\|x\|_2 \leq 1$  but with no continuous derivative at when  $\|x\|_2 = 1$  and  $\|x\|_2 = 0$ [9]. From the premise where we all know that an integral operator can smooth a function. The idea around construction of compactly supported radial basis function with a given smoothness is to not only use an integral operator acting on the truncate power function  $\phi_\ell$  but also to adjust the size of  $\ell$  to ensure positive definiteness. Because of radial symmetry, all operations can be reduced to univariate operation and considering only the integral operator on the right-half real line, then extending to the other half of the real line before generalizing to higher dimensional space. The usual bone of contention is the kind of integral operator to be used for high-dimensional problems. Wendland's functions (compactly supported radial basis functions of minimal degree) are the most popular of all compactly supported radial basis functions. Now, let us take a look at the construction of Wendland's functions. First, let us consider the following integral operator

$$(\mathcal{I}\phi)(r) := \int_r^\infty t \phi(t) dt, \text{ for } r \geq 0, \quad (17)$$

which was first introduced in the context of constructing compactly supported radial basis functions[10] but got less smooth functions in higher dimensional space  $\mathcal{R}^d$ . Using this

operator in a more elegant way by repeatedly applying  $\mathcal{I}$  on Ashkey's truncated power functions, Wendland achieved

$$\phi_{d,k}(r) = \mathcal{I}^k \phi_\ell, \text{ where } \ell = \lfloor \frac{d}{2} \rfloor + k + 1, \phi_\ell = (1 - \|x\|_2)_+^\ell. \quad (18)$$

using mathematical software,  $\phi_{d,k}(r)$  can be computed easily and can also be generally be represented as

$$\phi_{d,k}(r) = \mathcal{I}^k \phi_\ell = \phi_{\ell+k} p_{k,\ell}(r) = (1 - r)_+^{\lfloor \frac{d}{2} \rfloor + k + 1} p_{k,\ell}(r), \quad (19)$$

where  $p_{k,\ell}(r)$  is polynomial of degree  $k$  whose coefficients depends on  $\ell$ . For this project, we have used the Wendland function  $\phi_{d,k}(r)$  when  $d = 3$  and  $k = 0$  i.e.

$$\phi_{d,k}(r) = \phi_{3,0}(r) = (1 - r)_+^2 \quad (20)$$

where  $r$  represents 2-d euclidean norm  $r = \|(x, y) - (x_i, y_i)\|$ .

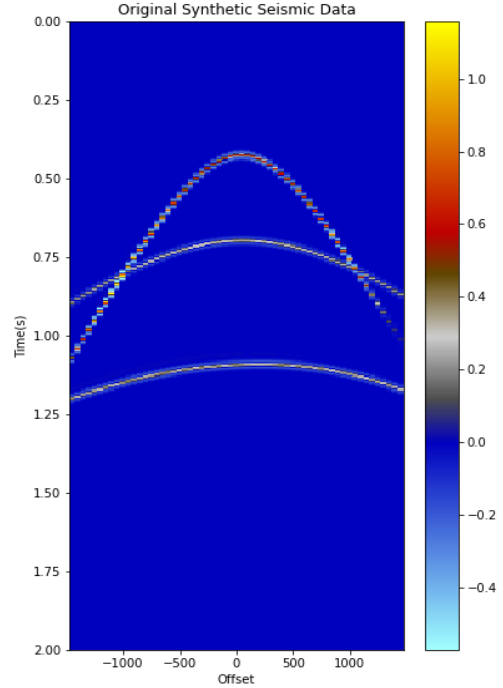
### 3. DATASET

We used two different gathered shots for this project, a synthetic seismic data, and a real seismic data. A shot gather can be represented as a 2-D matrix. The vertical axis represents the two-way travel time of the travelling seismic waves, while the horizontal axis represents the offset (distance between seismic source and receivers). Each column is called a seismic trace (amplitudes at a certain offset for the entire recording time of seismic shooting). The synthetic gathered shots have 60 traces and 501 time steps (0 - 2 seconds) while the real data has 2001 time steps (0 - 4 seconds) and 96 traces. To demonstrate a real world approach to seismic data interpolation, we would be omitting traces in steps of 10 from 10% till 90% of the entire traces and interpolating the missing traces with different techniques.

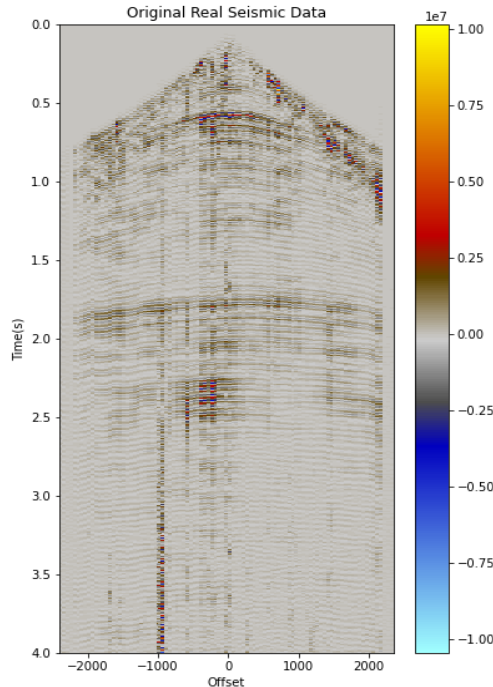
### 4. RESULTS AND DISCUSSION

We start the test by running the interpolation techniques on synthetic data with missing traces before testing with real seismic data. A plot of both synthetic and real seismic data is shown in fig 1. The synthetic seismic data is shown in figure 1a while the real seismic plot is shown in figure 1b

The result using RBF interpolation on synthetic data can be found from figure 2 to figure 10 and on real data from figure 11 to figure 19 while the result from using k-nearest-neighbour can be seen from figure 20 to figure 28 for synthetic data and from figure 29 to figure 37 for real data. A juxtaposition of the performance of knn and rbf interpolation can be seen in figure 38a for synthetic data and figure 38b for real seismic data. A plausible observation is that the PSNR decreases with increasing percentage of decimated traces in both interpolation technique but that of RBF performs better since it generally has higher PSNR. Looking at the figure 10c



(a) Synthetic Seismic Data



(b) Real Seismic Data

**Fig. 1:** A plot showing trace amplitude values for (a) Synthetic and (b) Real seismic shot gathers

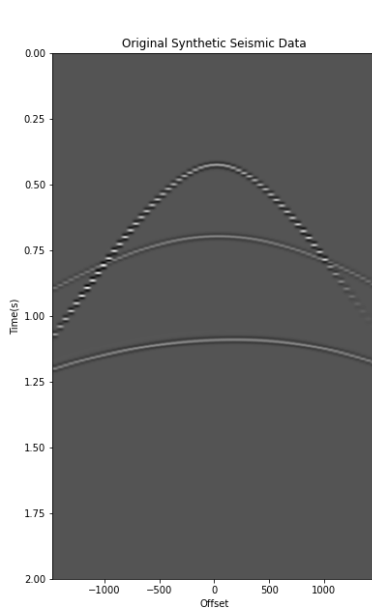
and comparing with figure 28b it is also palpable that RBF interpolation works best. This validation also comes corroborated with 2D FFT plot between the interpolated and original data as seen in the figures below.

## 5. CONCLUSION AND FUTURE WORK

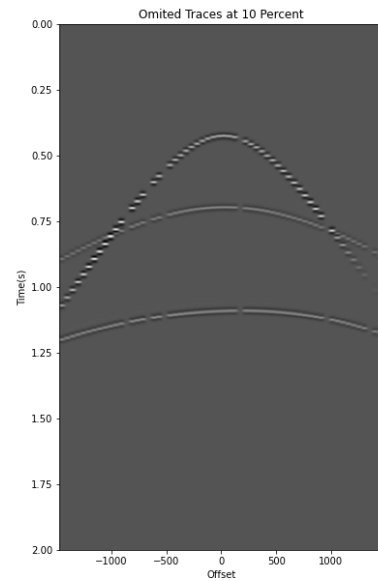
We have used RBF interpolation techniques to fill in missing traces of seismic data, a solution to a germane problem in mostly oil and gas industry. We have also been able to deduce that RBF interpolation works better than KNN interpolation. A major drawback of this interpolation technique is that it requires the calculation of an interpolant which is usually restricted to a specific dataset. This means this interpolation technique would not generalize. One advantage is that new methods like the use of deep neural networks could create a model that could generalize to multiple datasets and RBF interpolation could be used in preprocessing before being passed to such networks.

## 6. REFERENCES

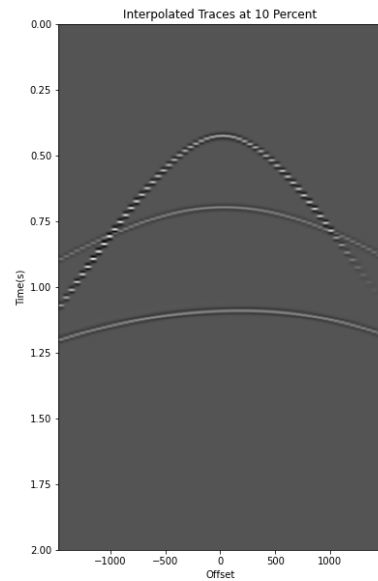
- [1] Sergey Fomel, “Seismic reflection data interpolation with differential offset and shot continuation,” *Geophysics*, vol. 68, no. 2, pp. 733–744, 2003.
- [2] Simon Spitz, “Seismic trace interpolation in the  $f_x$  domain,” *Geophysics*, vol. 56, no. 6, pp. 785–794, 1991.
- [3] Mostafa Naghizadeh and Mauricio D Sacchi, “ $f_x$  adaptive seismic-trace interpolation,” *Geophysics*, vol. 74, no. 1, pp. V9–V16, 2009.
- [4] Sheng Xu, Yu Zhang, Don Pham, and Gilles Lambaré, “Antileakage fourier transform for seismic data regularization,” *Geophysics*, vol. 70, no. 4, pp. V87–V95, 2005.
- [5] Nira Dyn, David Levin, and Samuel Rippa, “Numerical procedures for surface fitting of scattered data by radial functions,” *SIAM Journal on Scientific and Statistical Computing*, vol. 7, no. 2, pp. 639–659, 1986.
- [6] Liu Yang Zhang Mi, “Seismic data interpolation based on radial basis function,” *IGC*, vol. 20, no. 5, pp. 435–439, 2017.
- [7] Vaclav Skala, “A practical use of radial basis functions interpolation and approximation,” *Investigacion Operacional*, vol. 37, no. 5, pp. 137–145, 2016.
- [8] Wilna Du Toit, *Radial basis function interpolation*, Ph.D. thesis, Stellenbosch: Stellenbosch University, 2008.
- [9] Shengxin Zhu, “Compactly supported radial basis functions: how and why?,” 2012.
- [10] Zongmin Wu, “Compactly supported positive definite radial functions,” *Advances in computational mathematics*, vol. 4, no. 1, pp. 283–292, 1995.



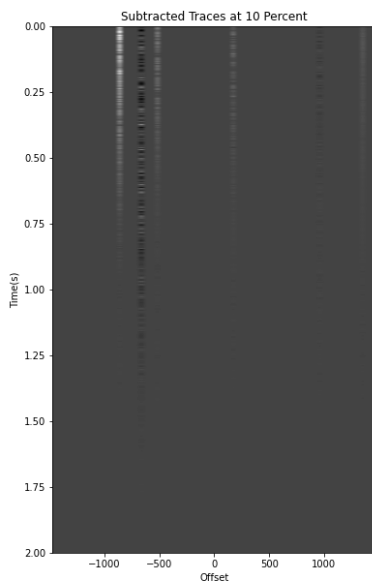
(a) Original Synthetic Seismic Data



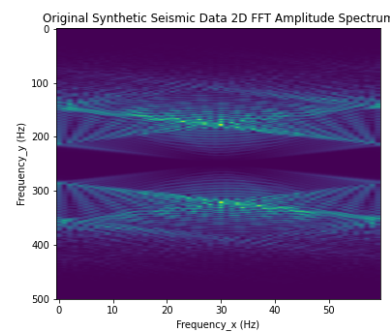
(b) Decimated Data with 10% Traces Missing



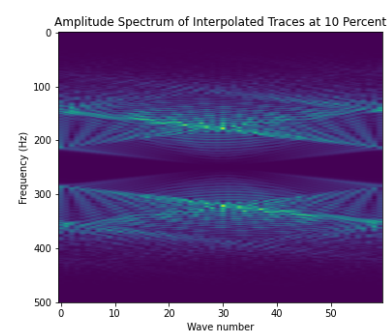
(c) Reconstructed Seismic Data After Interpolation



(d) Reconstruction Error



(e) Original Synthetic Seismic Data 2D FFT



(f) Reconstructed Synthetic Seismic Data 2D FFT

**Fig. 2:** RBF Result on Synthetic Data at 10% Omitted Traces.

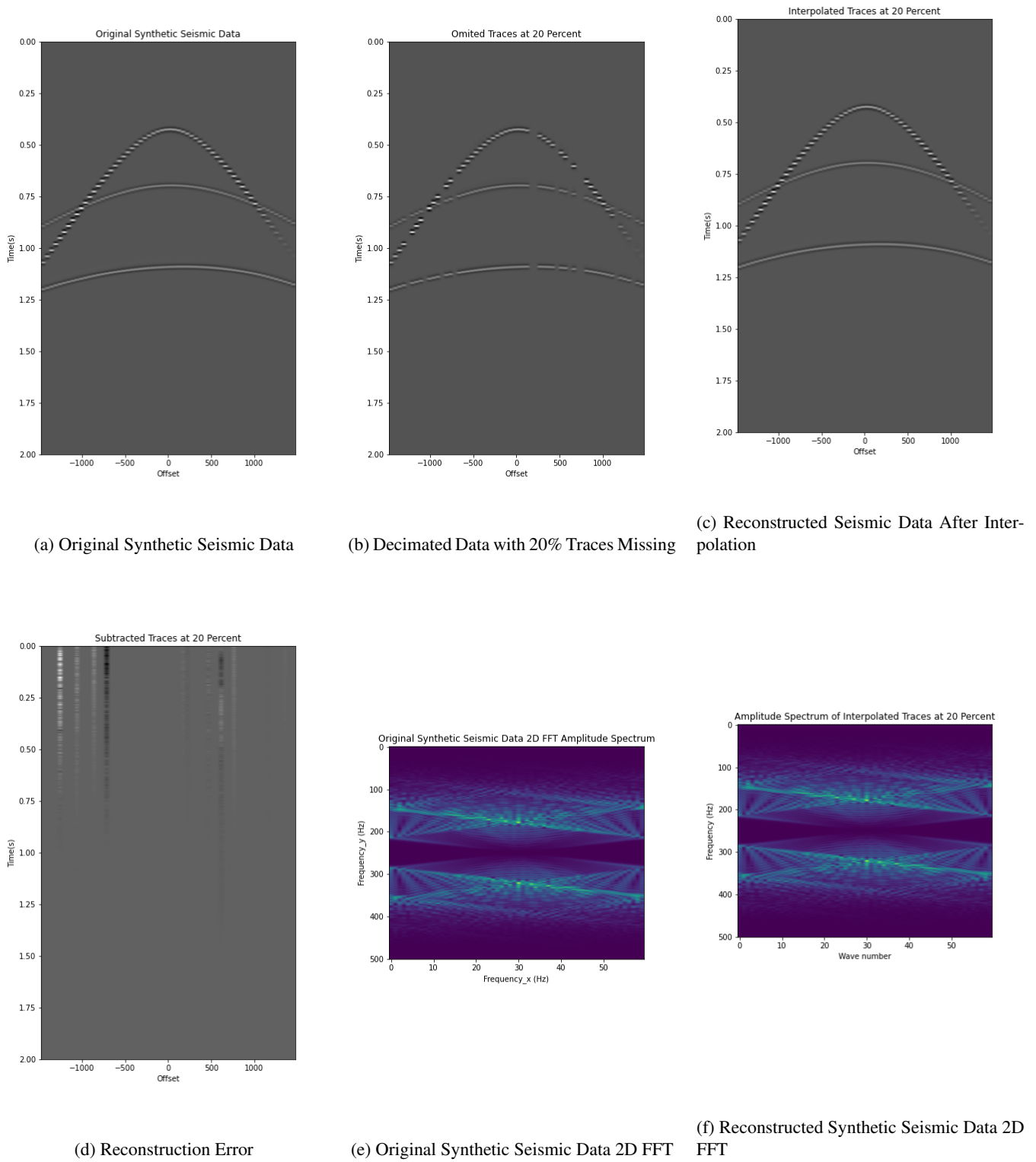


**Fig. 3:** RBF Result on Synthetic Data at 20% Omitted Traces.

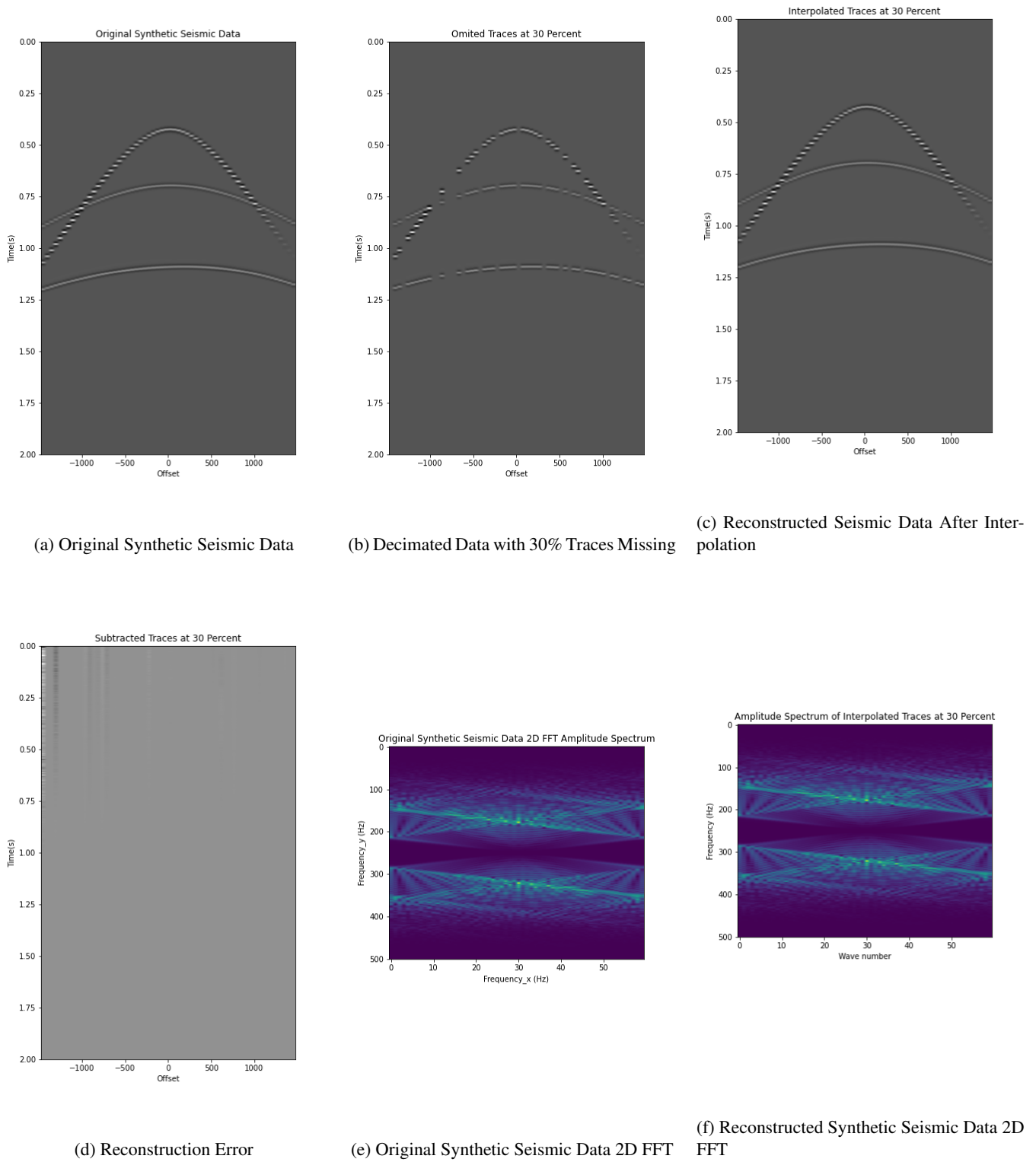


**Fig. 4:** RBF Result on Synthetic Data at 30% Omitted Traces.

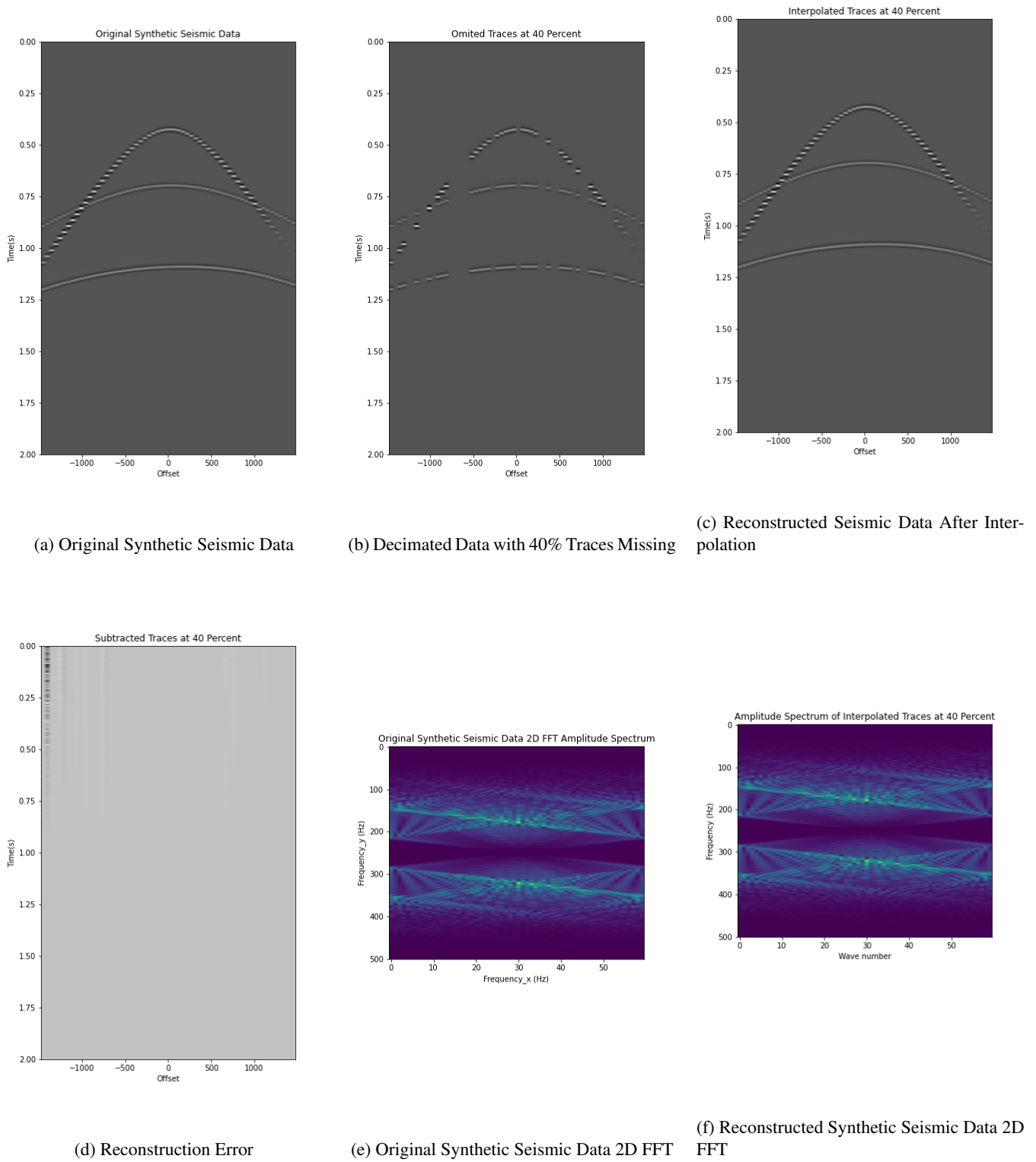


**Fig. 5:** RBF Result on Synthetic Data at 40% Omitted Traces.

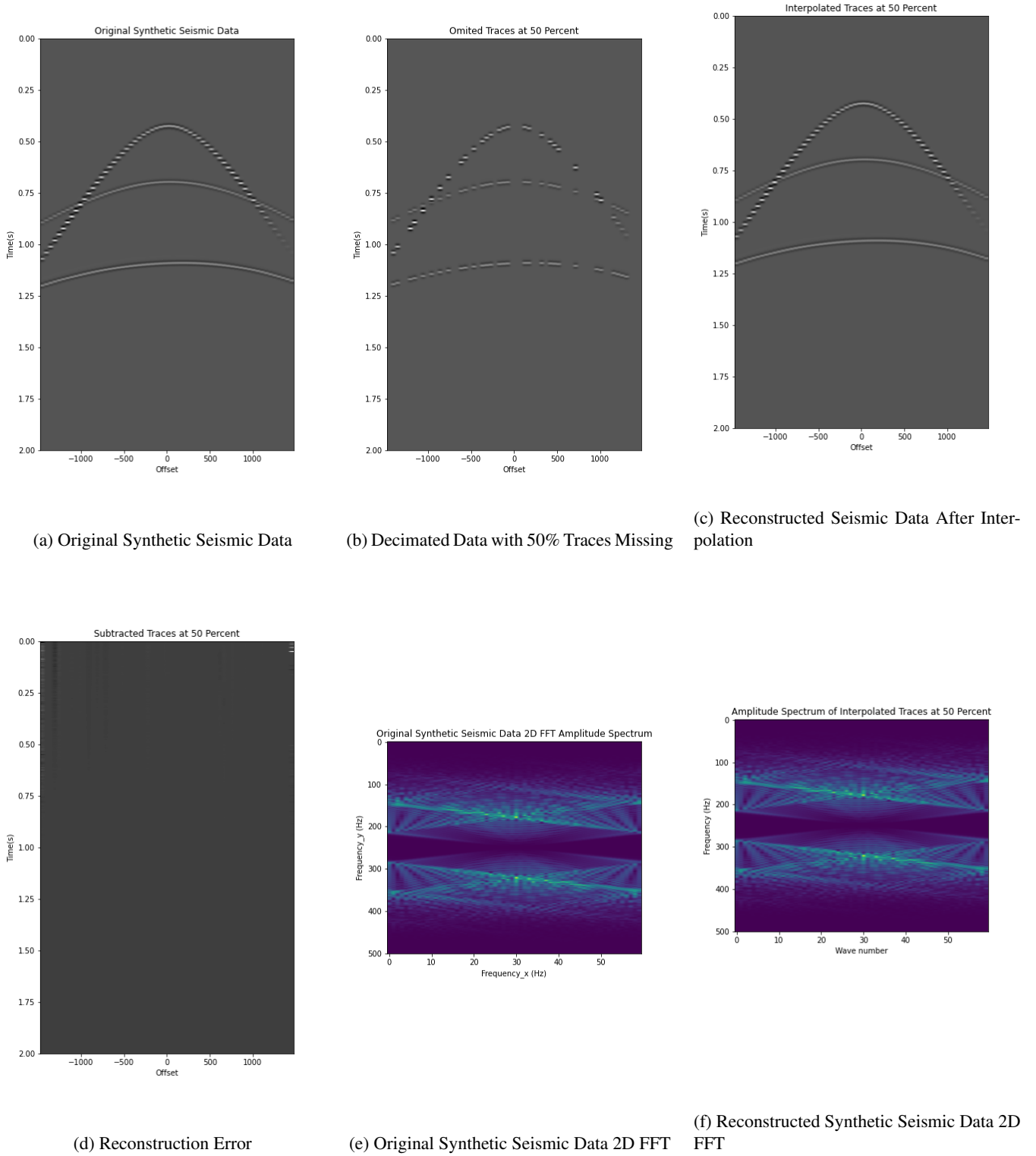


**Fig. 6:** RBF Result on Synthetic Data at 50% Omitted Traces.

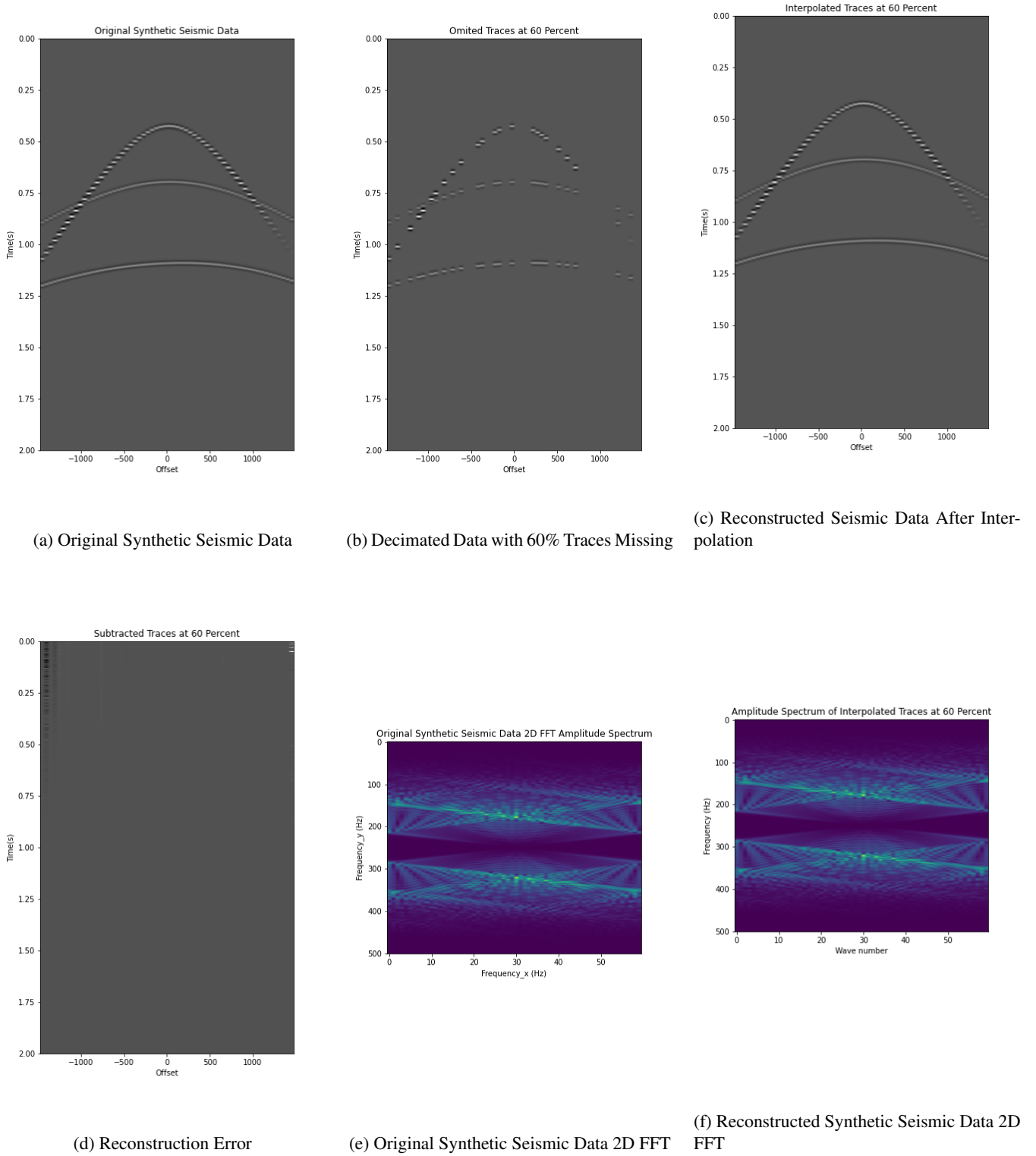


**Fig. 7:** RBF Result on Synthetic Data at 60% Omitted Traces.

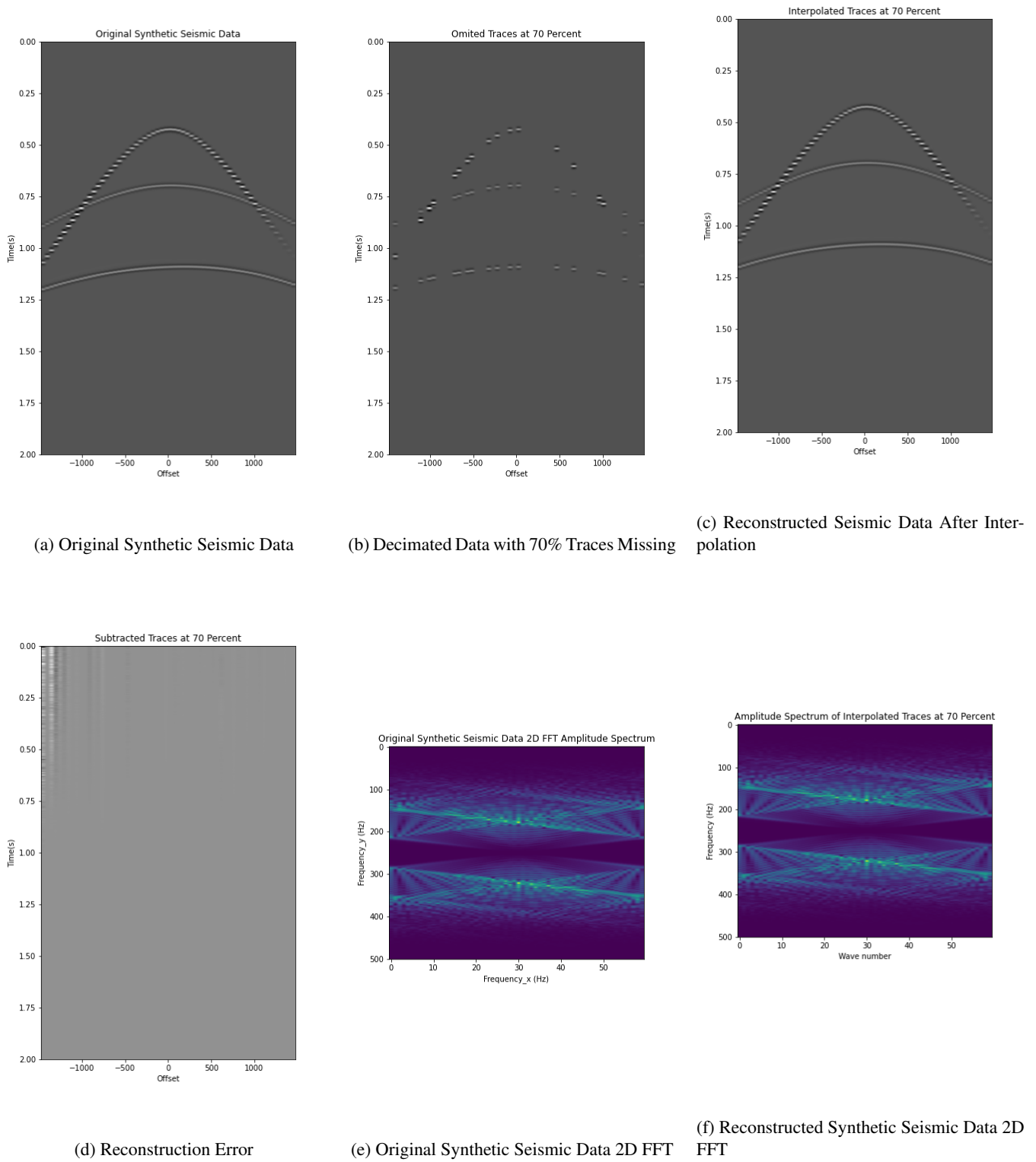


**Fig. 8:** RBF Result on Synthetic Data at 70% Omitted Traces.

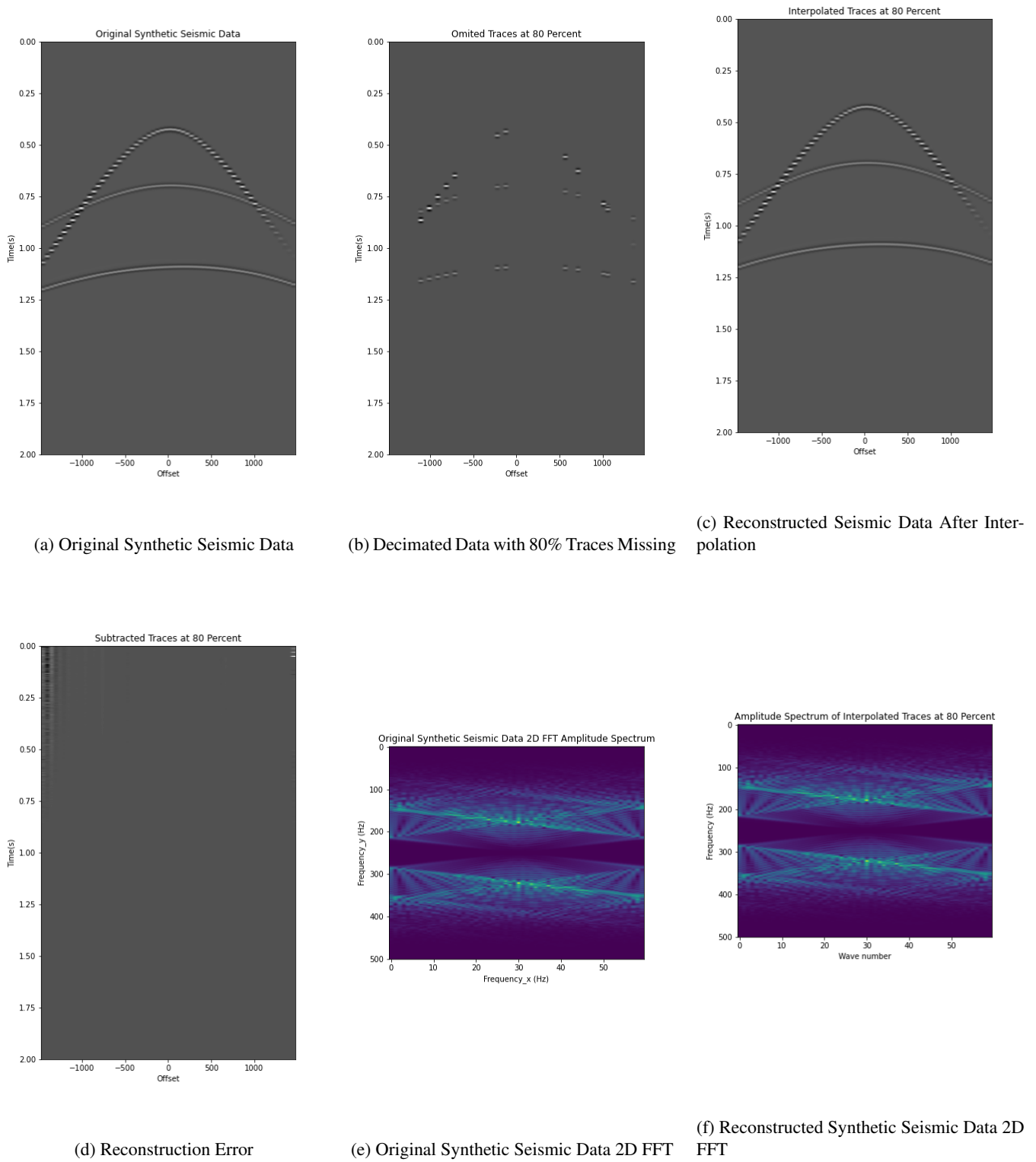


**Fig. 9:** RBF Result on Synthetic Data at 80% Omitted Traces.

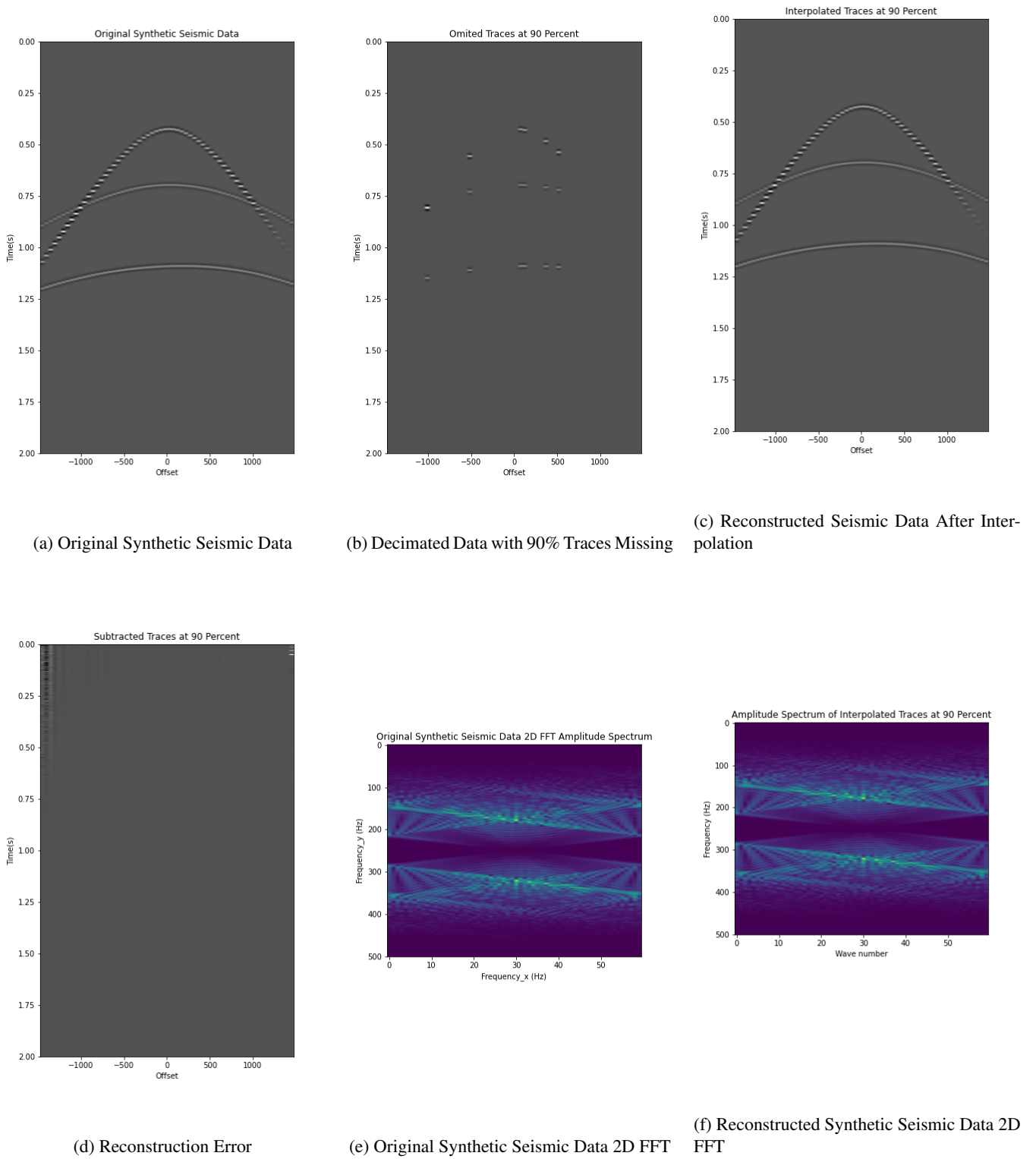


**Fig. 10:** RBF Result on Synthetic Data at 90% Omitted Traces.

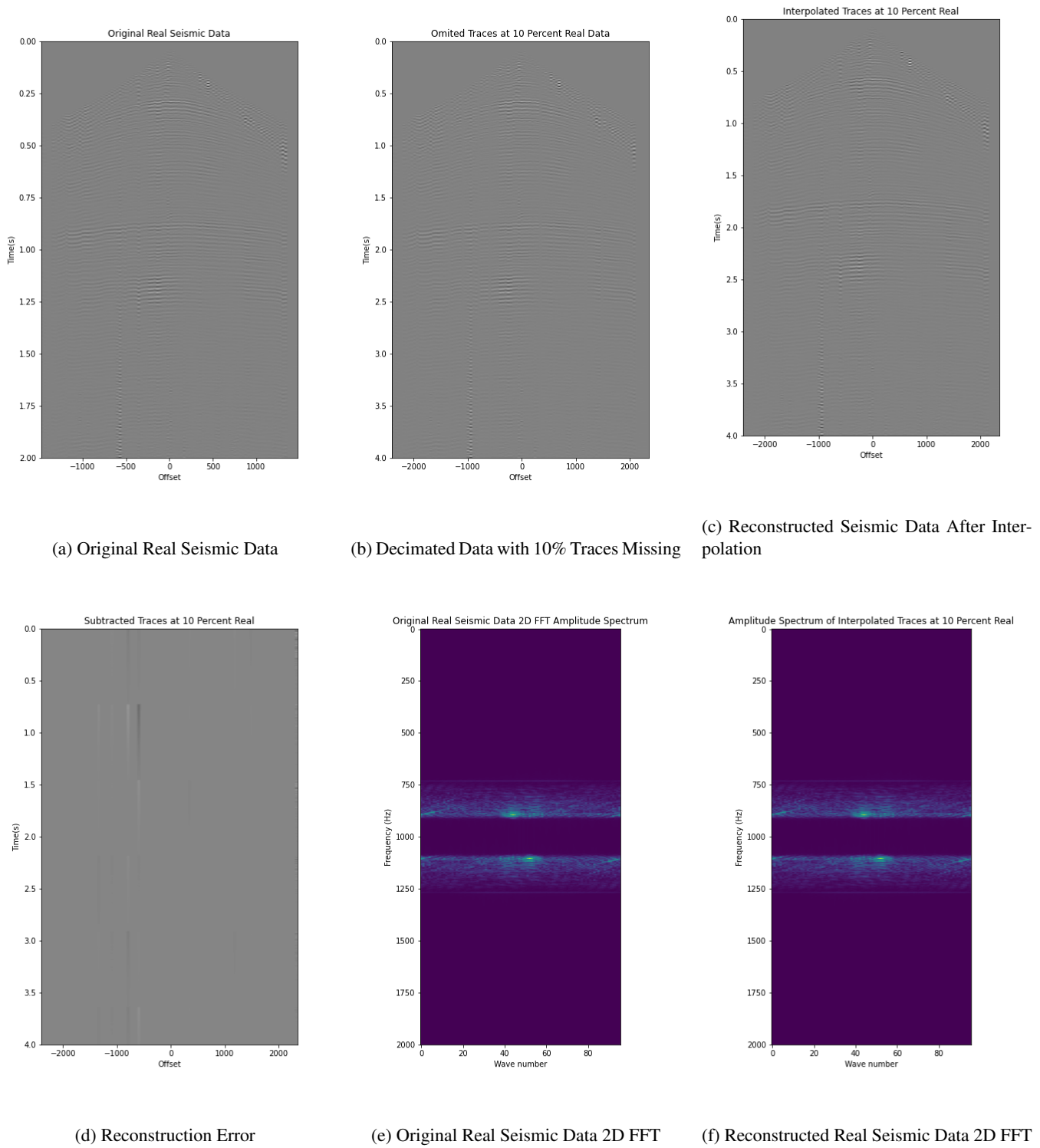


**Fig. 11:** RBF Result on Real Data at 10% Omitted Traces.

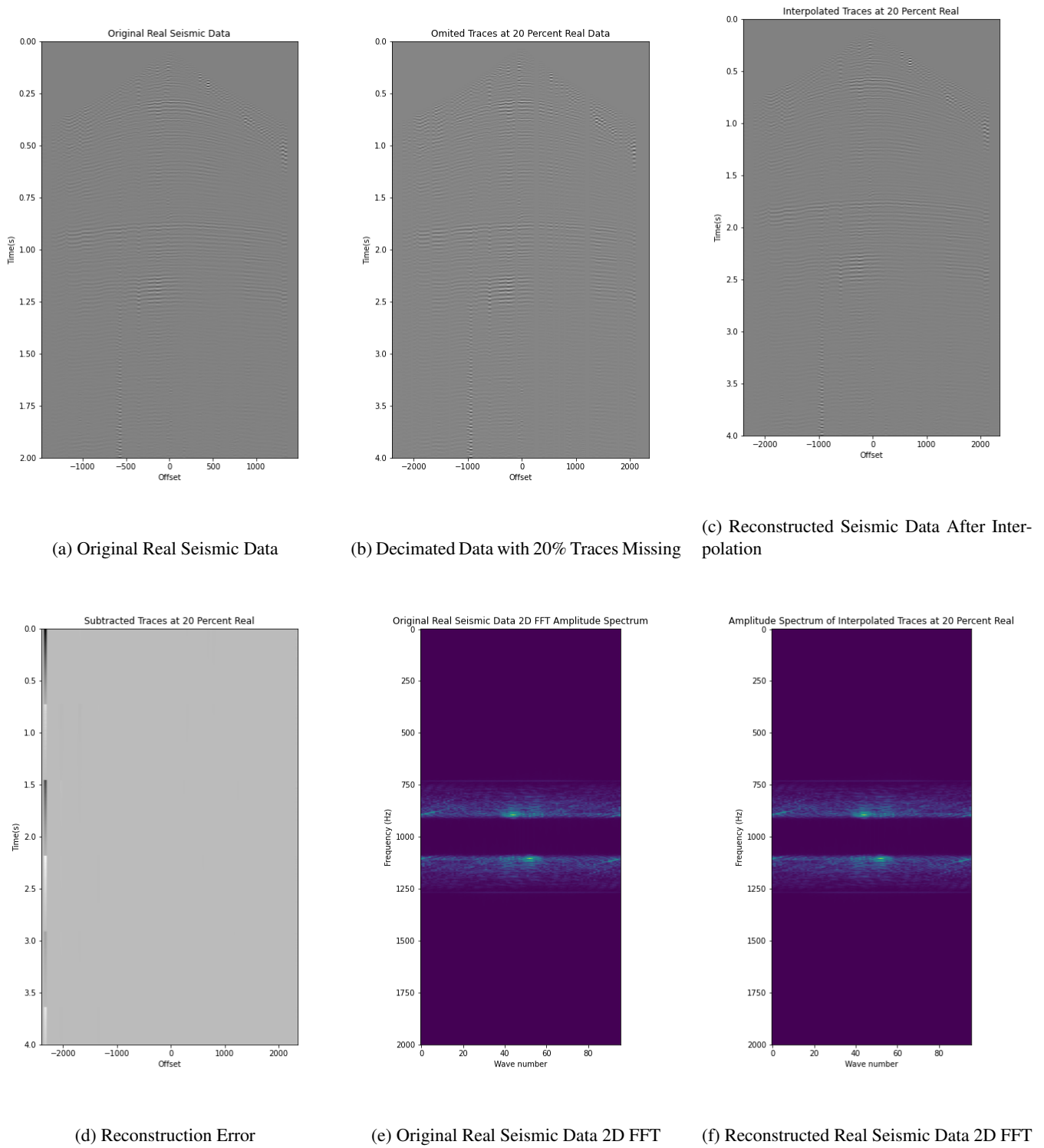


**Fig. 12:** RBF Result on Real Data at 20% Omitted Traces.

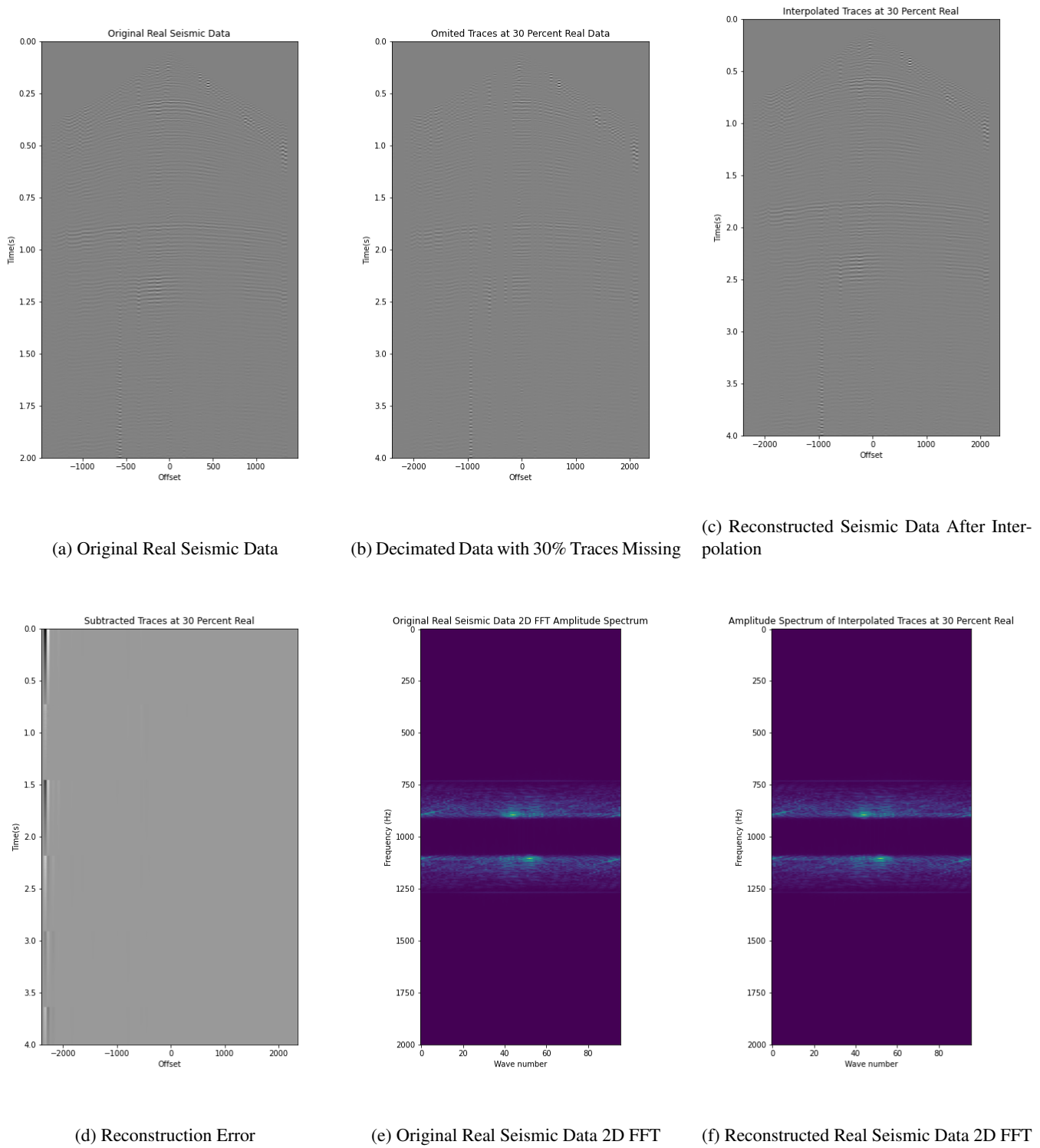


**Fig. 13:** RBF Result on Real Data at 30% Omitted Traces.

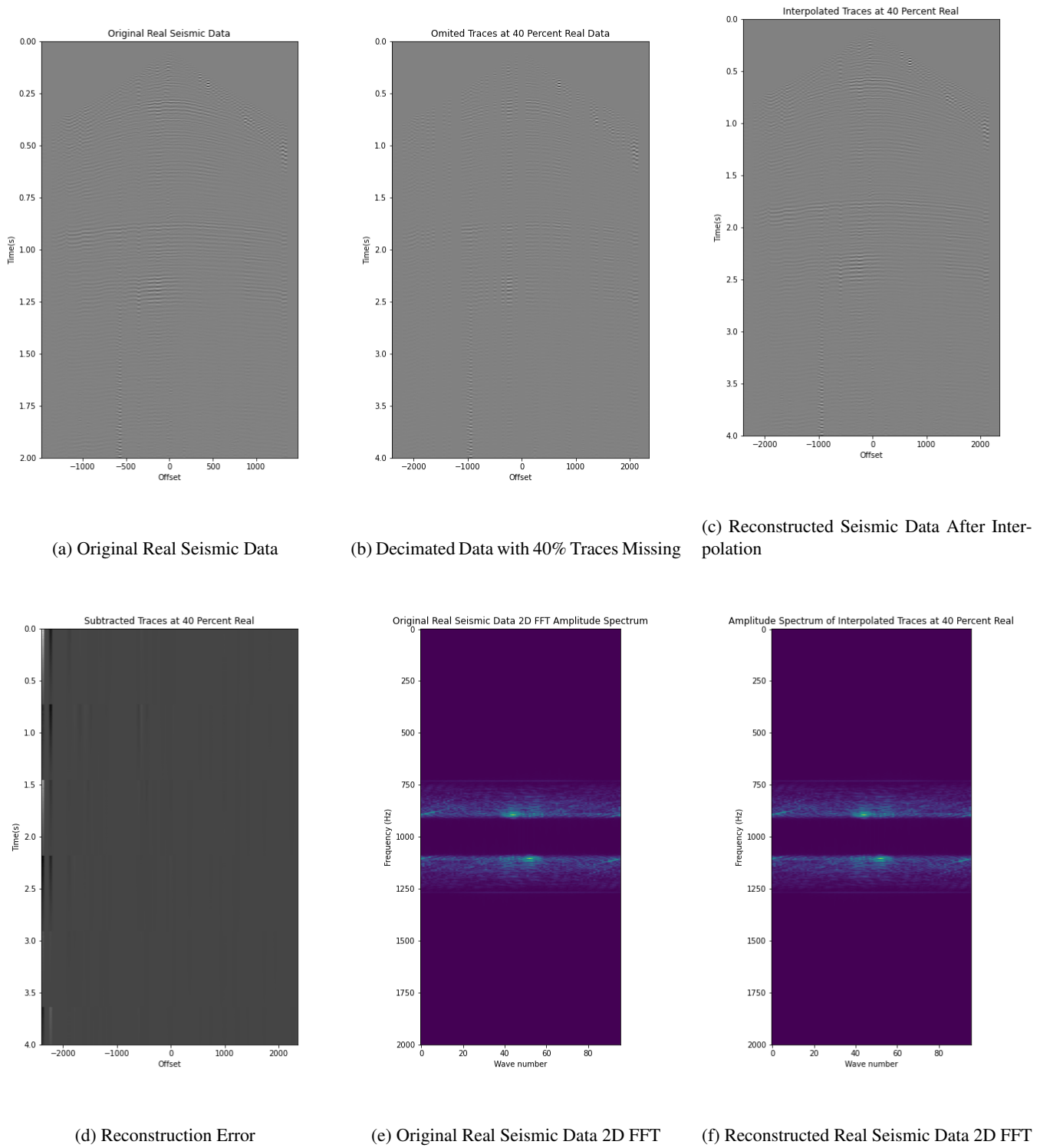


**Fig. 14:** RBF Result on Real Data at 40% Omitted Traces.

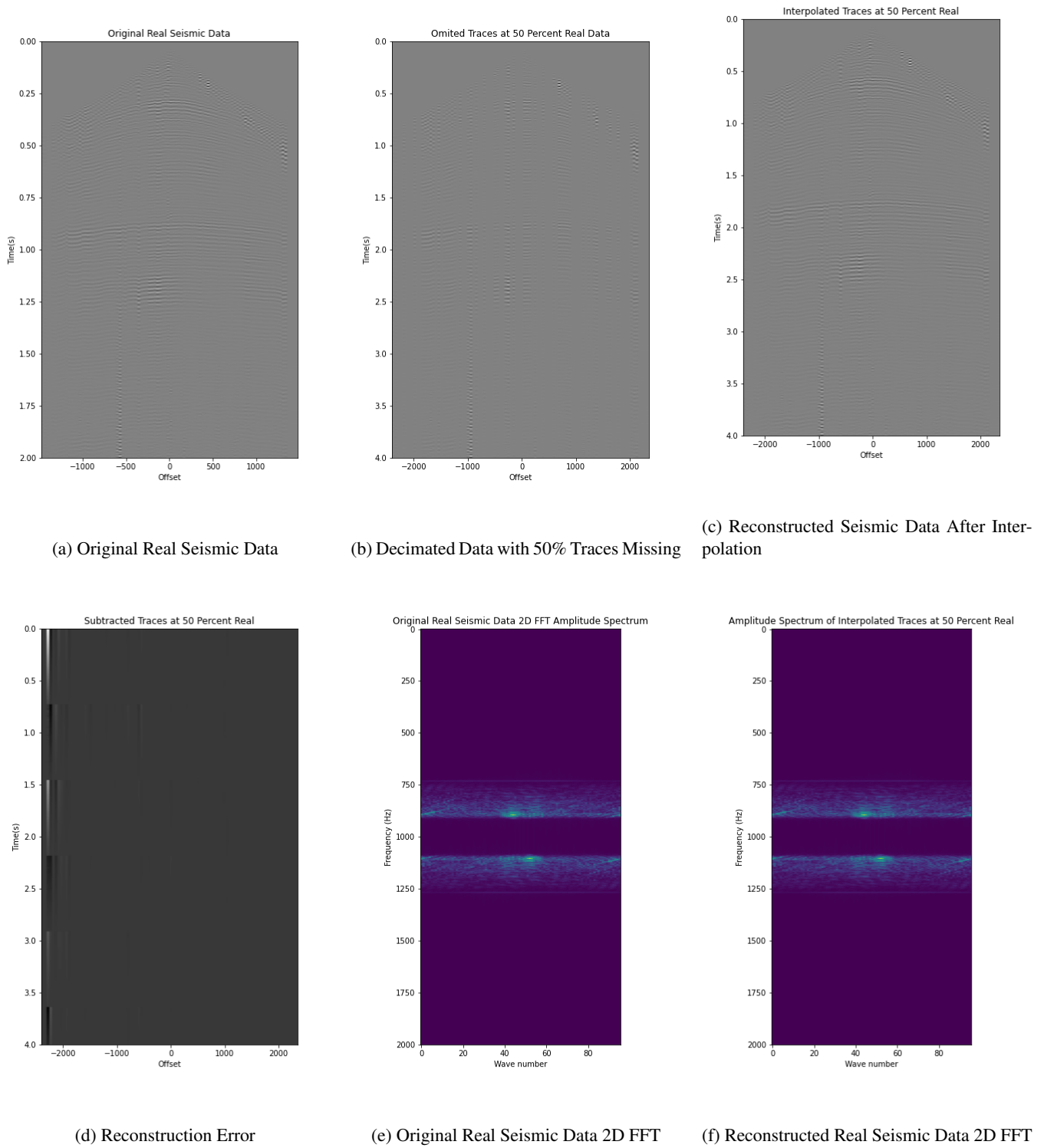


**Fig. 15:** RBF Result on Real Data at 50% Omitted Traces.

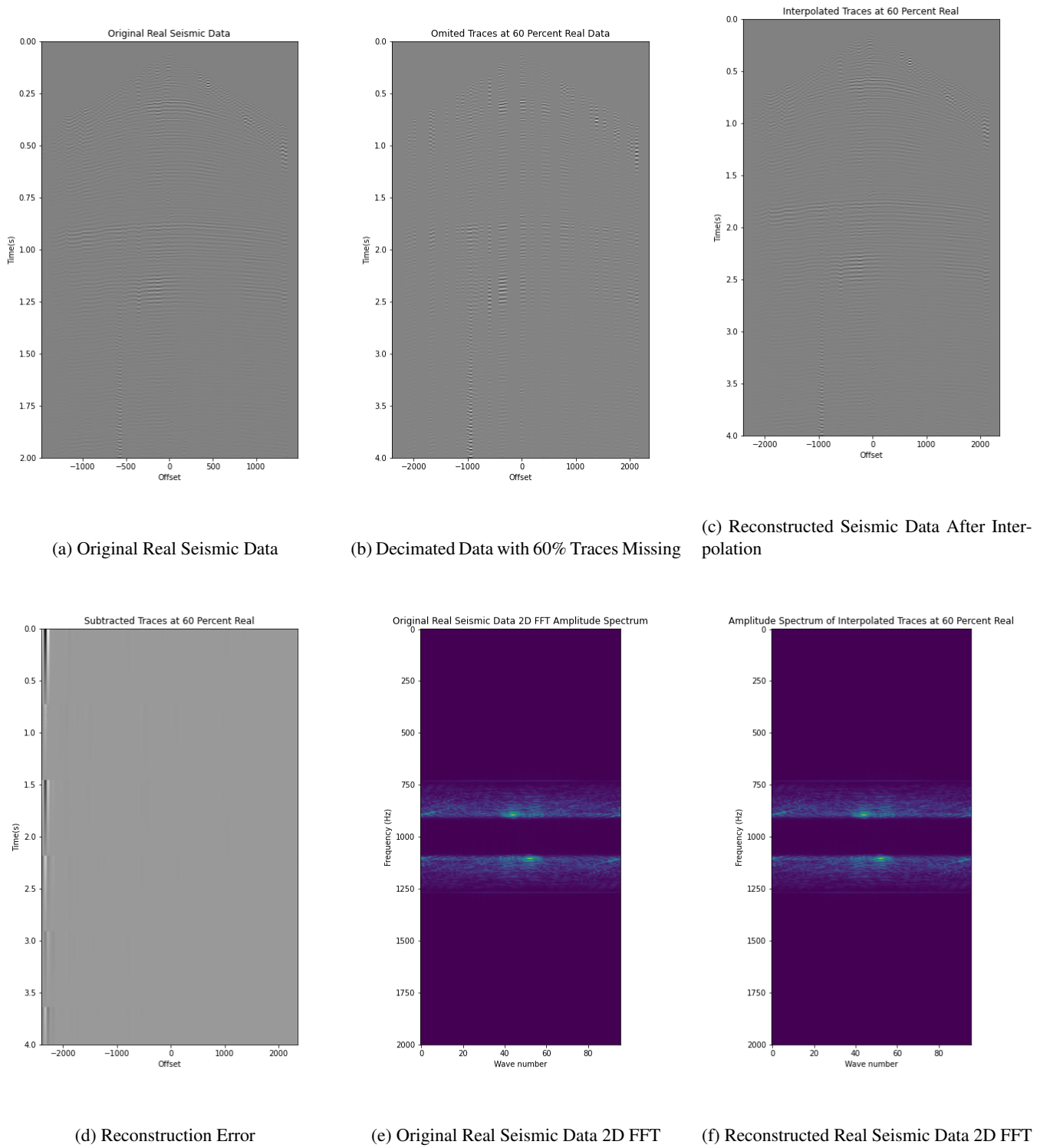


**Fig. 16:** RBF Result on Real Data at 60% Omitted Traces.

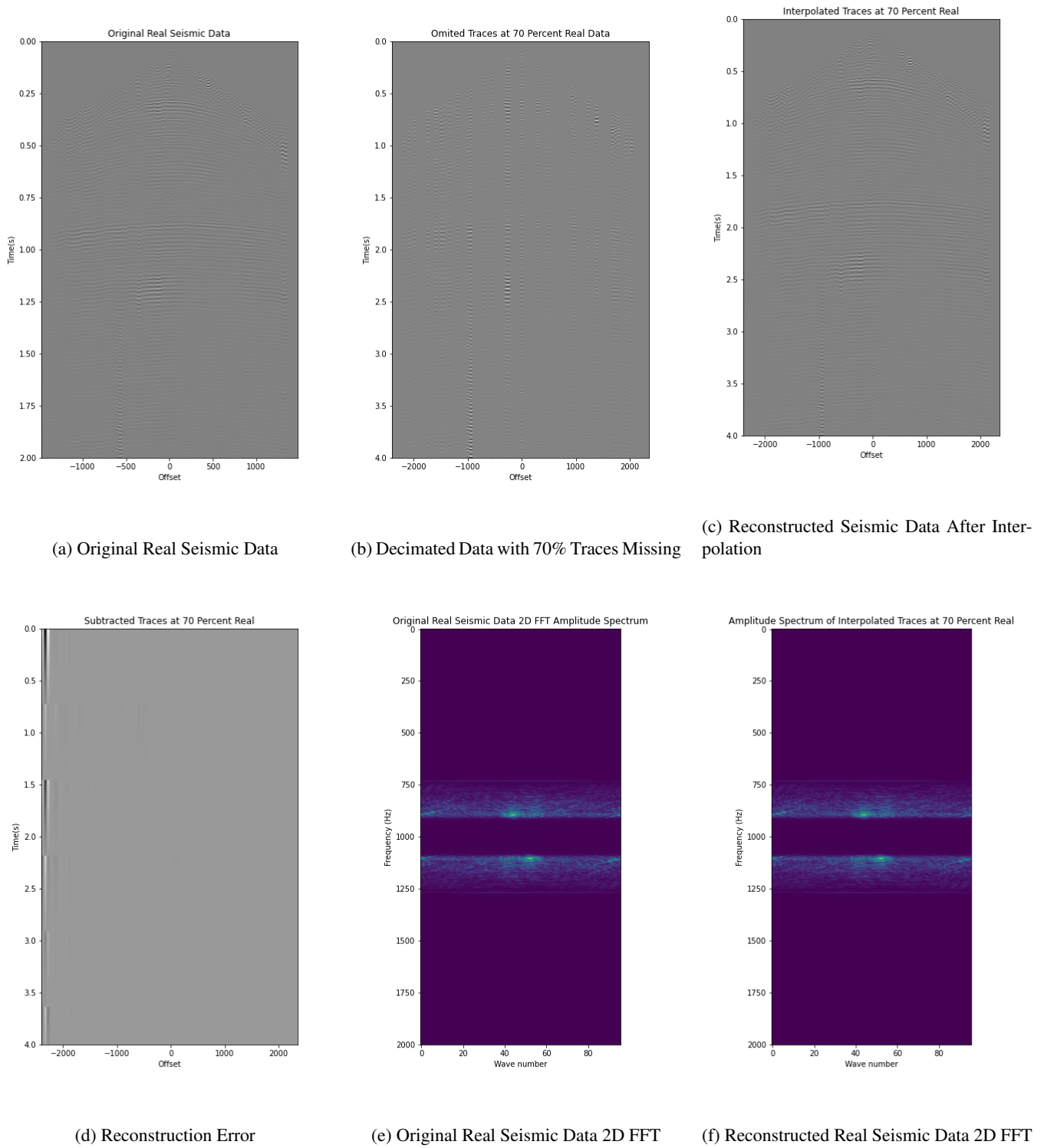


**Fig. 17:** RBF Result on Real Data at 70% Omitted Traces.

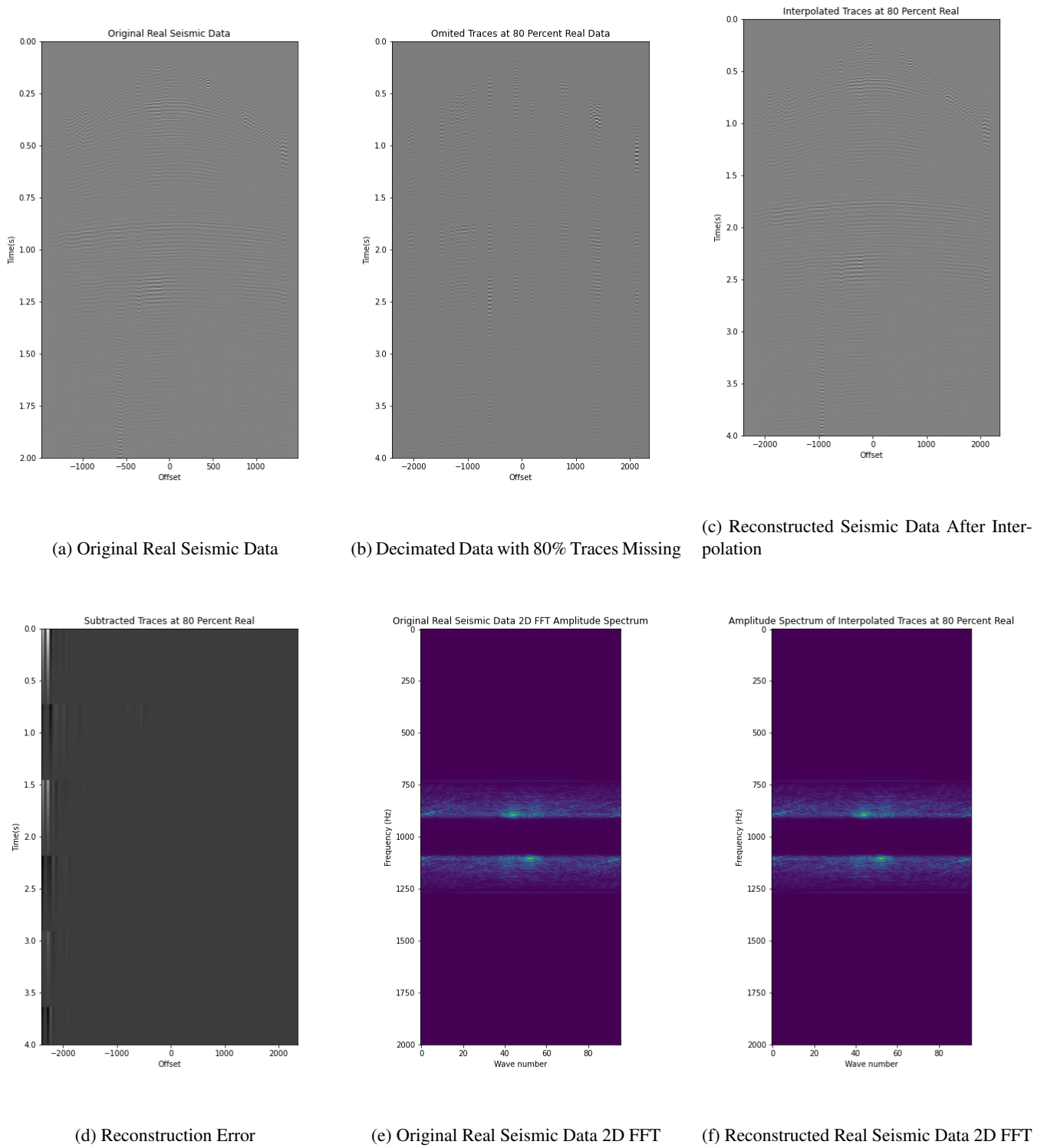


**Fig. 18:** RBF Result on Real Data at 80% Omitted Traces.

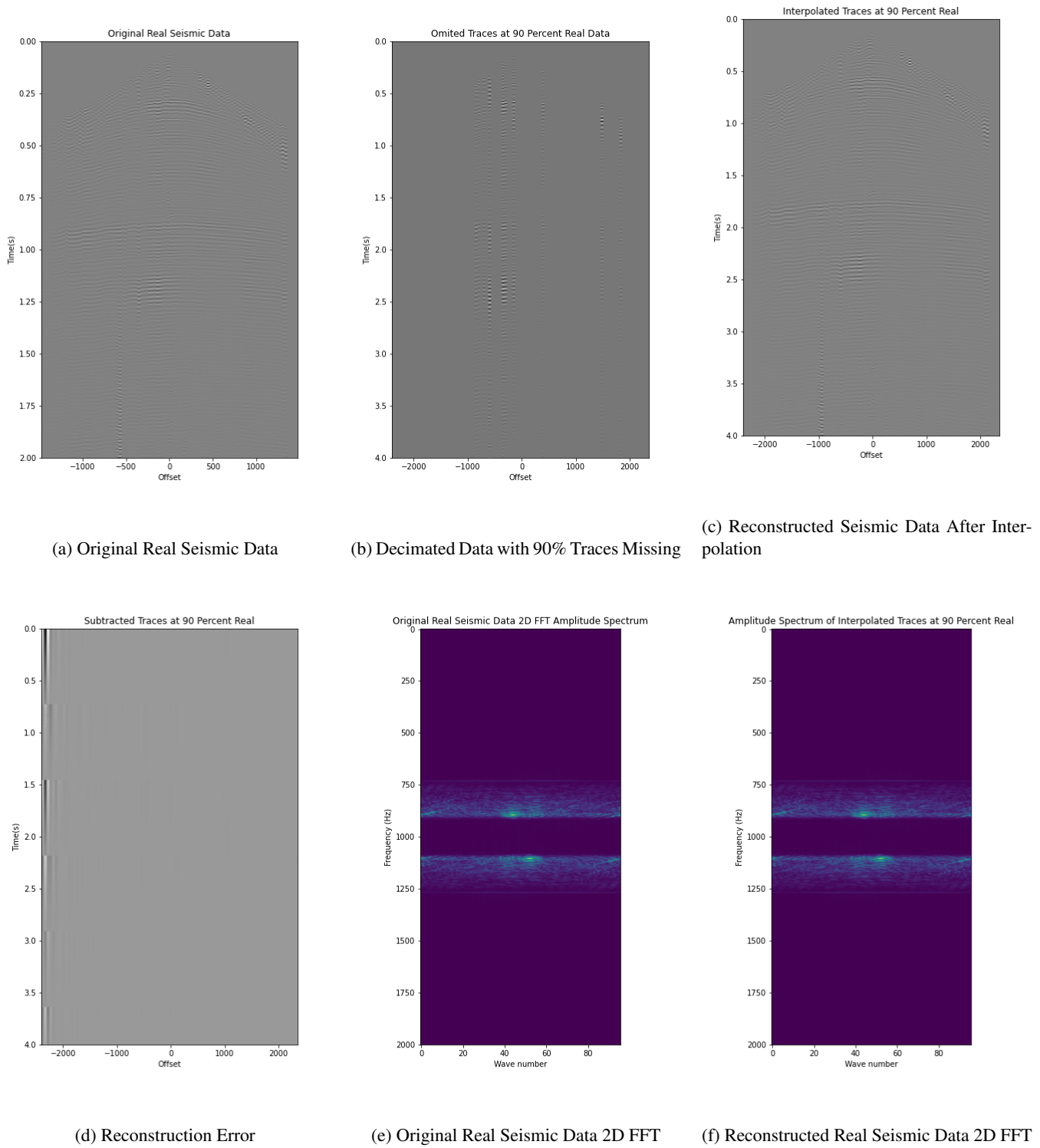
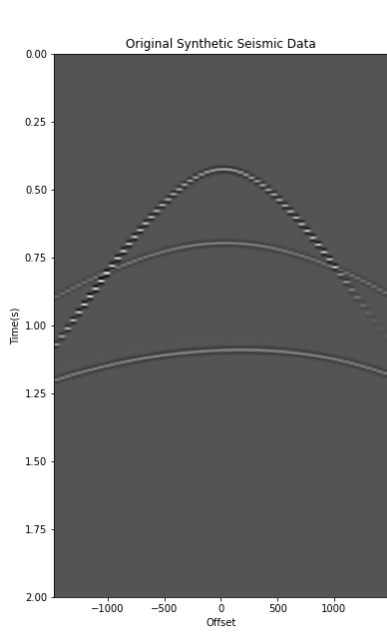
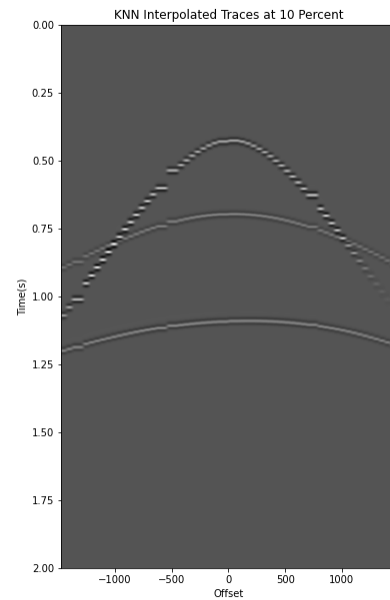


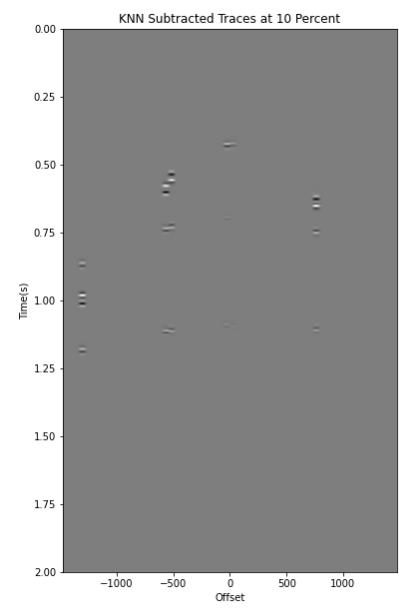
**Fig. 19:** RBF Result on Real Data at 90% Omitted Traces.



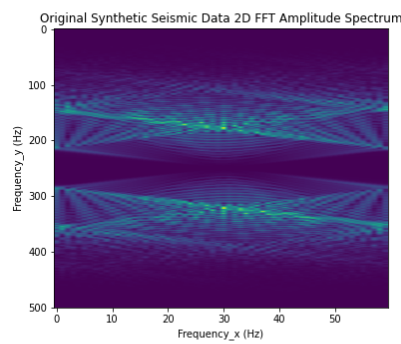
(a) Original Synthetic Seismic Data



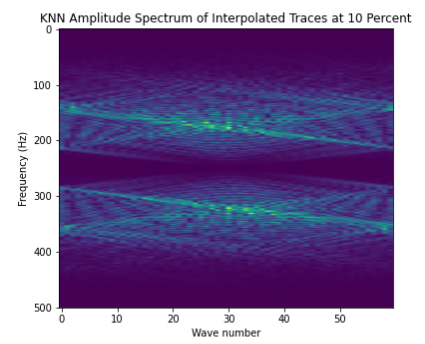
(b) Reconstructed Seismic Data After Interpolation



(c) Reconstruction Error

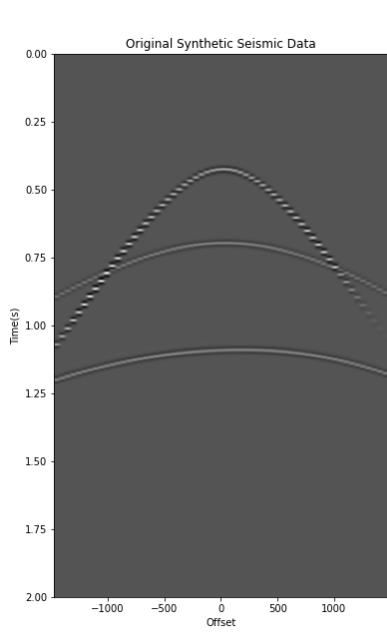


(d) Original Seismic Data 2D FFT

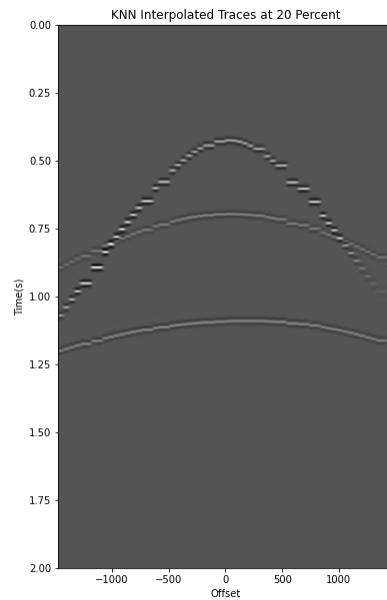


(e) Reconstructed Seismic Data 2D FFT

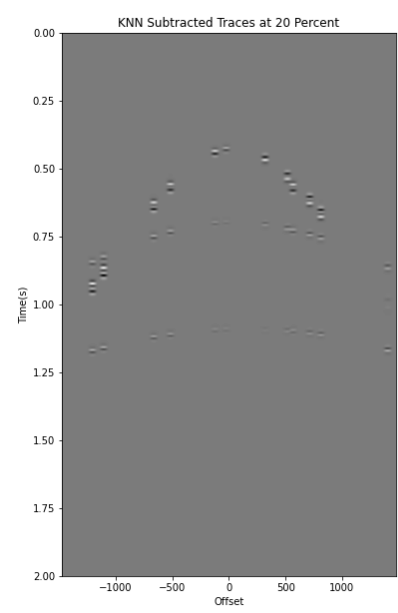
**Fig. 20:** KNN Result on Synthetic Data at 10% Omitted Traces.



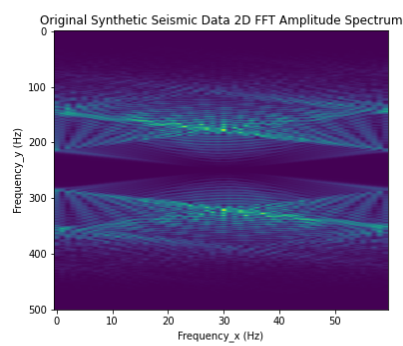
(a) Original Synthetic Seismic Data



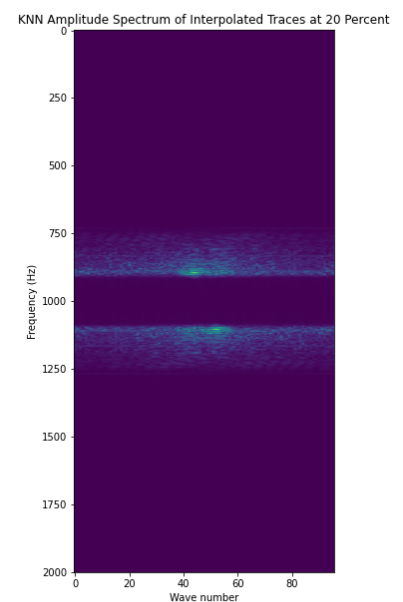
(b) Reconstructed Seismic Data After Interpolation



(c) Reconstruction Error

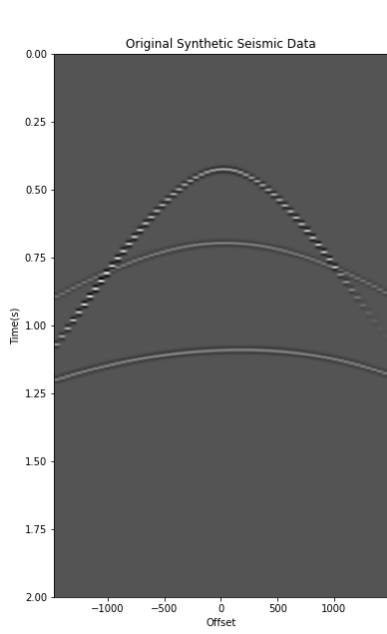


(d) Original Seismic Data 2D FFT

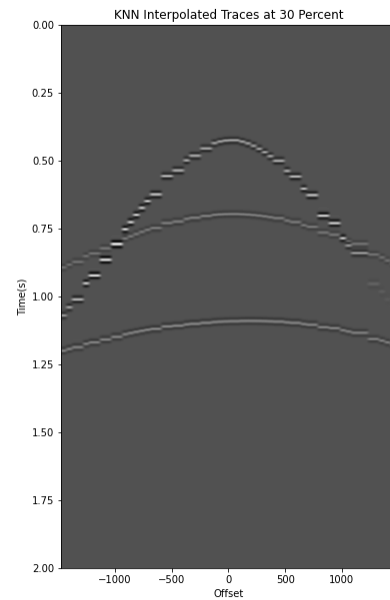


(e) Reconstructed Seismic Data 2D FFT

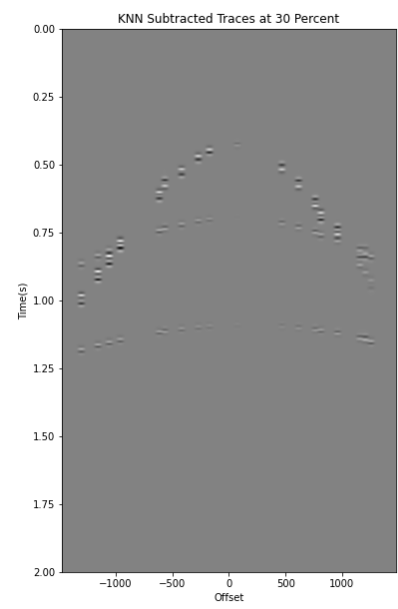
**Fig. 21:** KNN Result on Synthetic Data at 20% Omitted Traces.



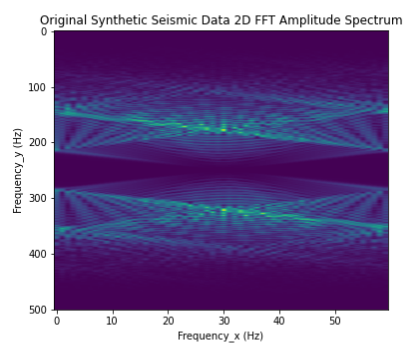
(a) Original Synthetic Seismic Data



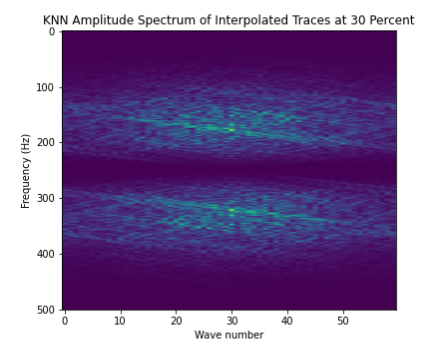
(b) Reconstructed Seismic Data After Interpolation



(c) Reconstruction Error

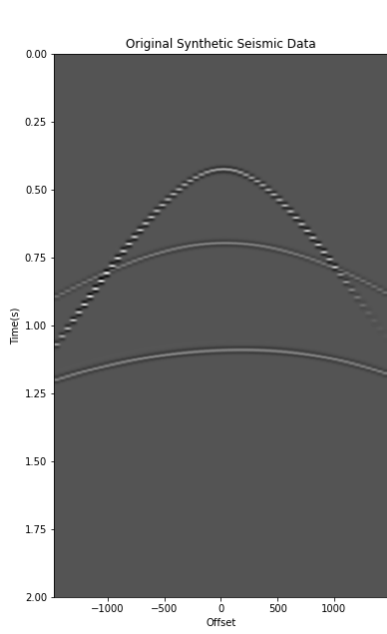


(d) Original Seismic Data 2D FFT

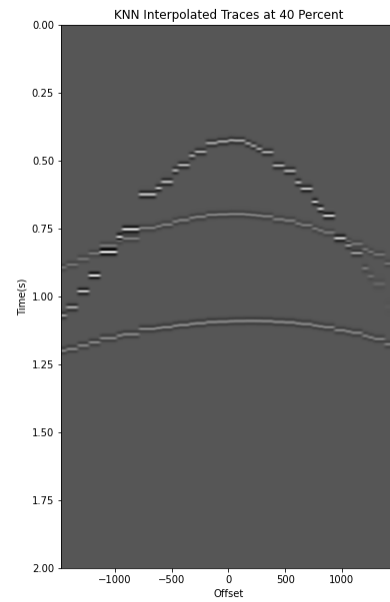


(e) Reconstructed Seismic Data 2D FFT

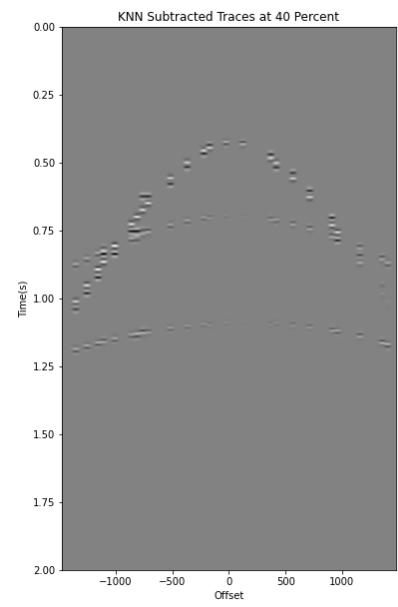
**Fig. 22:** KNN Result on Synthetic Data at 30% Omitted Traces.



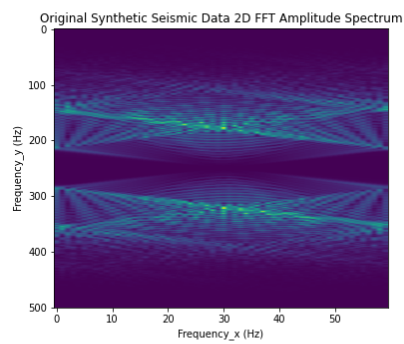
(a) Original Synthetic Seismic Data



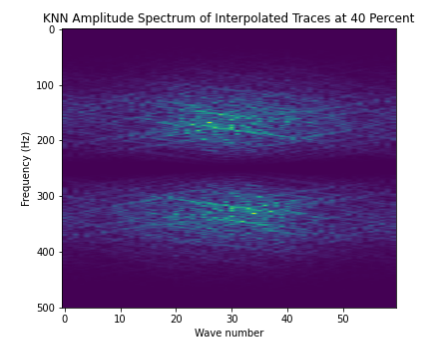
(b) Reconstructed Seismic Data After Interpolation



(c) Reconstruction Error

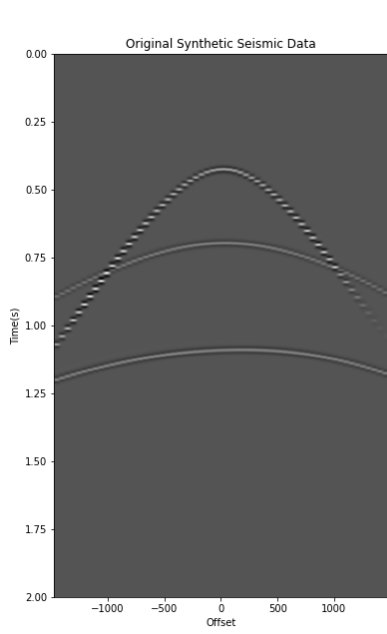


(d) Original Seismic Data 2D FFT

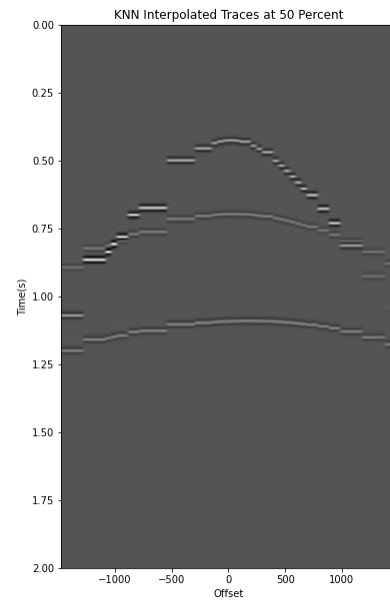


(e) Reconstructed Seismic Data 2D FFT

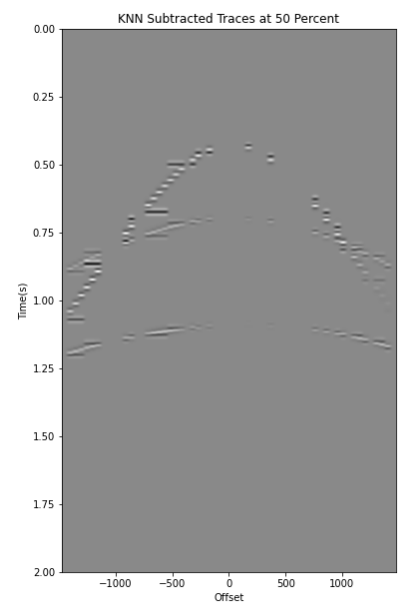
**Fig. 23:** KNN Result on Synthetic Data at 40% Omitted Traces.



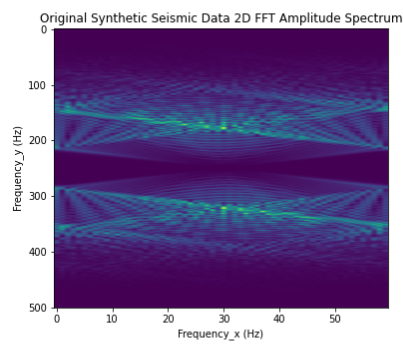
(a) Original Synthetic Seismic Data



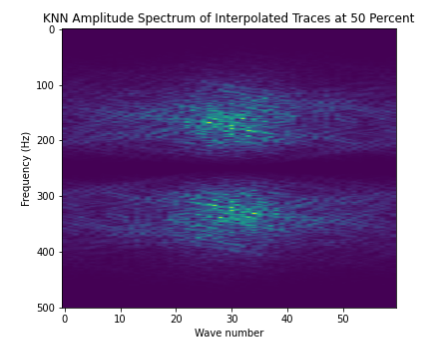
(b) Reconstructed Seismic Data After Interpolation



(c) Reconstruction Error

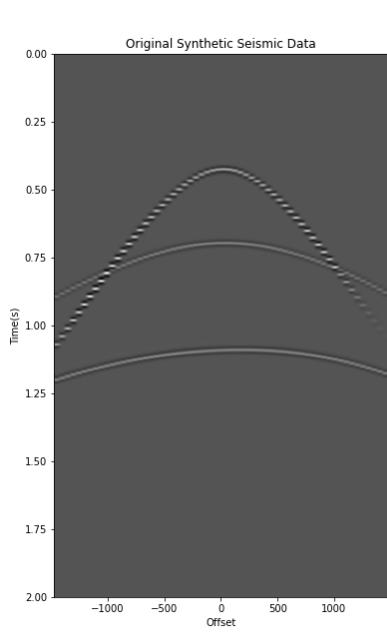


(d) Original Seismic Data 2D FFT

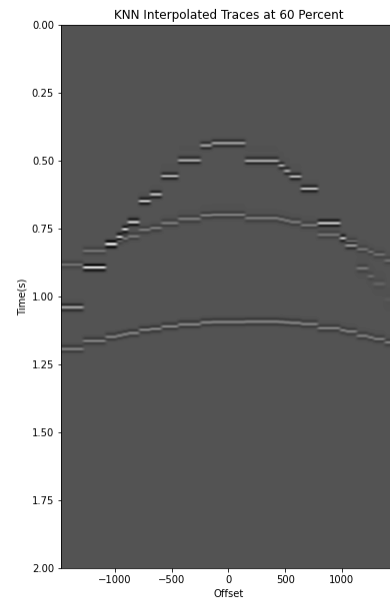


(e) Reconstructed Seismic Data 2D FFT

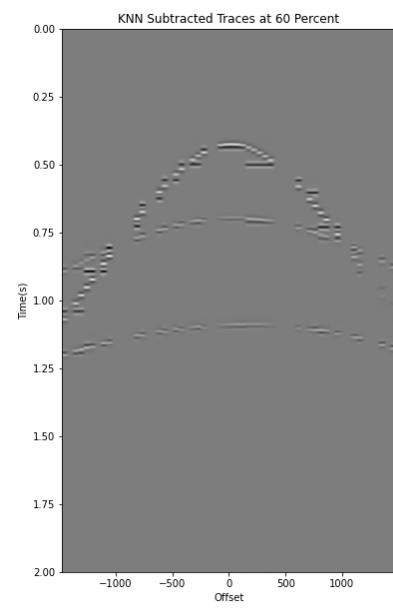
**Fig. 24:** KNN Result on Synthetic Data at 50% Omitted Traces.



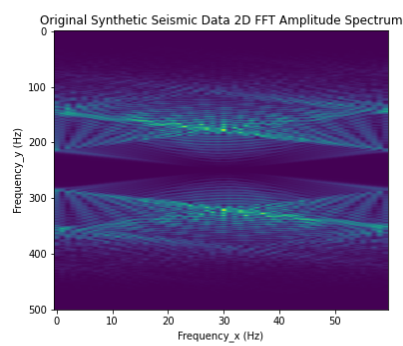
(a) Original Synthetic Seismic Data



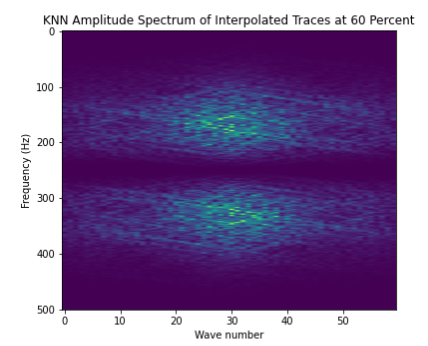
(b) Reconstructed Seismic Data After Interpolation



(c) Reconstruction Error

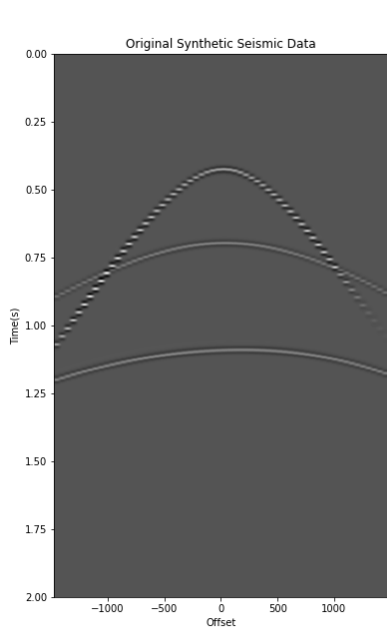


(d) Original Seismic Data 2D FFT

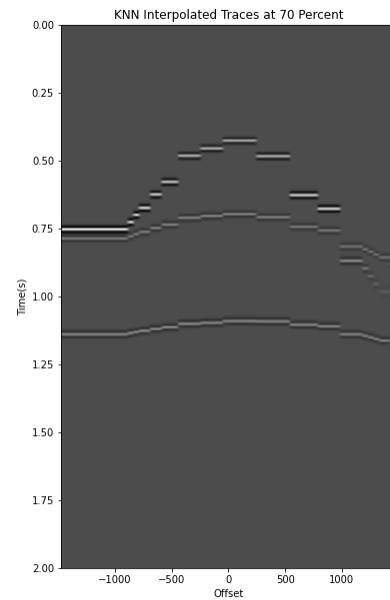


(e) Reconstructed Seismic Data 2D FFT

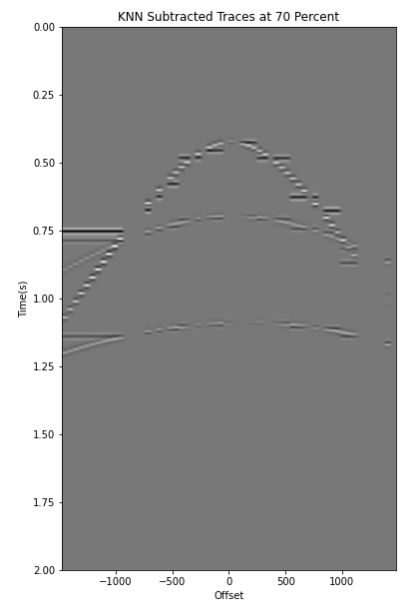
**Fig. 25:** KNN Result on Synthetic Data at 60% Omitted Traces.



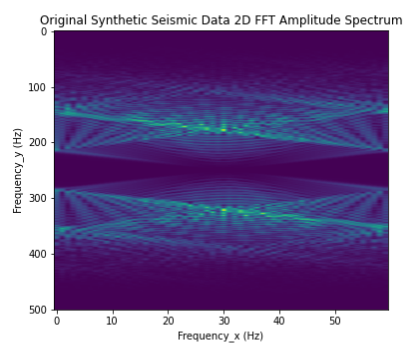
(a) Original Synthetic Seismic Data



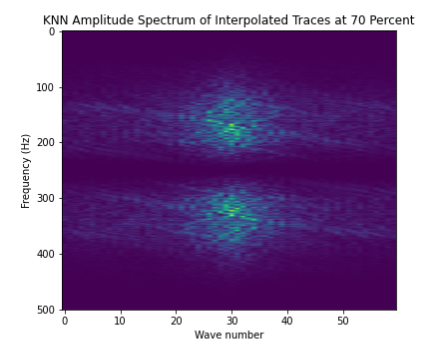
(b) Reconstructed Seismic Data After Interpolation



(c) Reconstruction Error

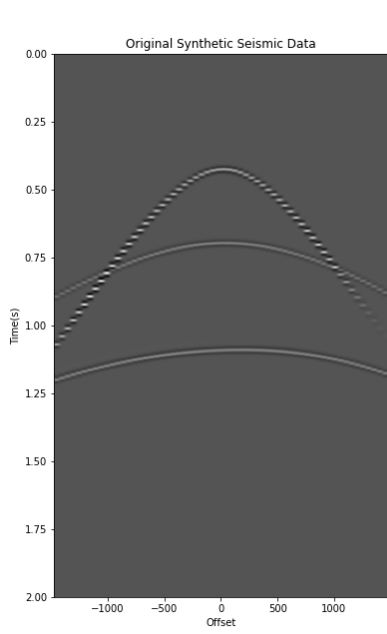


(d) Original Seismic Data 2D FFT

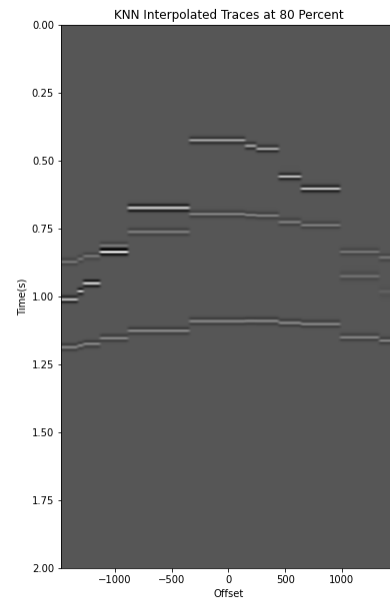


(e) Reconstructed Seismic Data 2D FFT

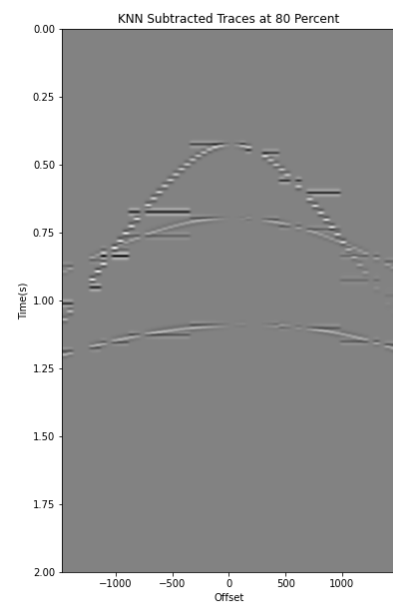
**Fig. 26:** KNN Result on Synthetic Data at 70% Omitted Traces.



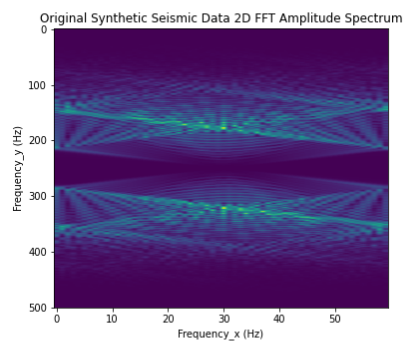
(a) Original Synthetic Seismic Data



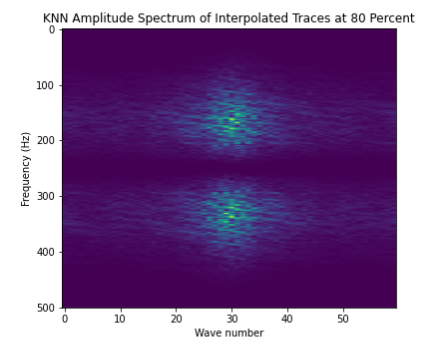
(b) Reconstructed Seismic Data After Interpolation



(c) Reconstruction Error

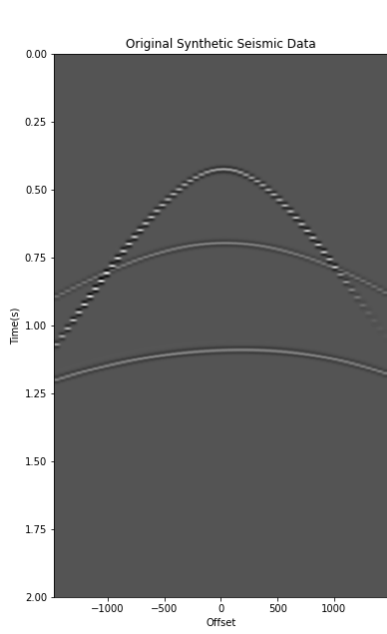


(d) Original Seismic Data 2D FFT

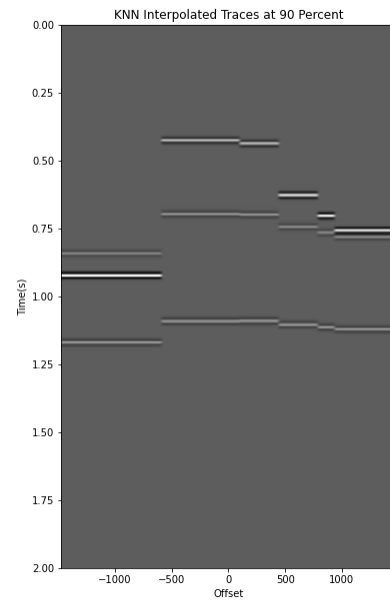


(e) Reconstructed Seismic Data 2D FFT

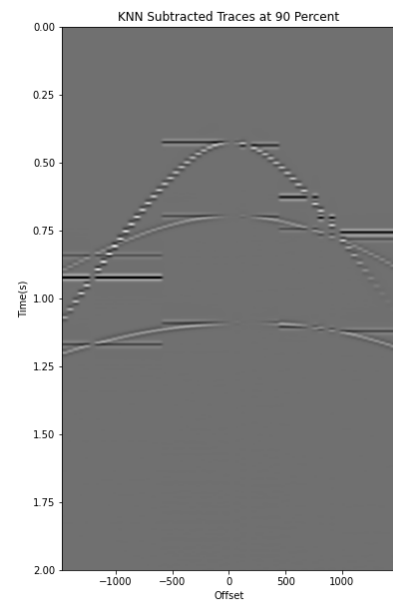
**Fig. 27:** KNN Result on Synthetic Data at 80% Omitted Traces.



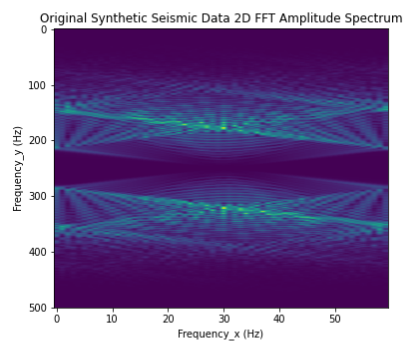
(a) Original Synthetic Seismic Data



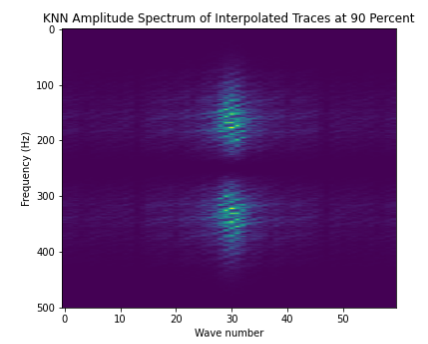
(b) Reconstructed Seismic Data After Interpolation



(c) Reconstruction Error

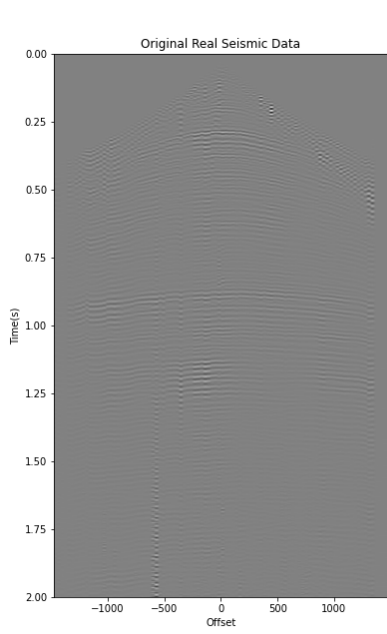


(d) Original Seismic Data 2D FFT

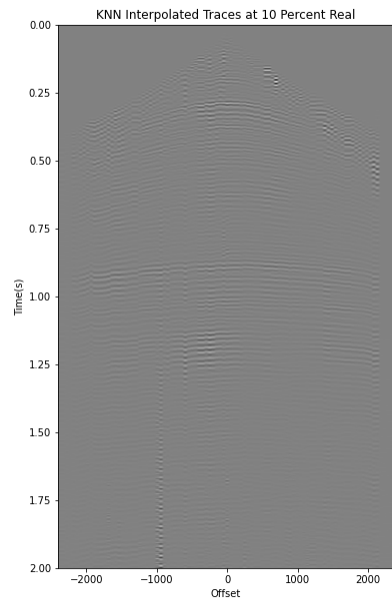


(e) Reconstructed Seismic Data 2D FFT

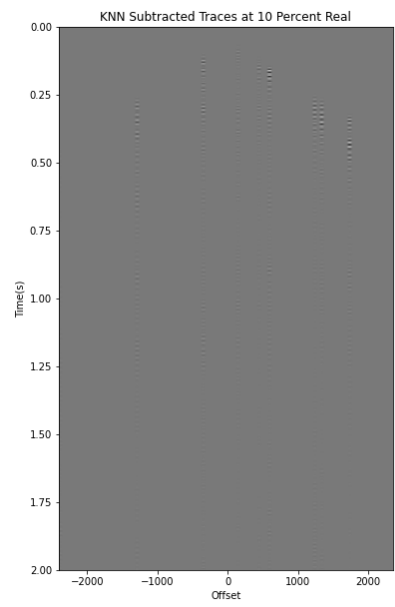
**Fig. 28:** KNN Result on Synthetic Data at 90% Omitted Traces.



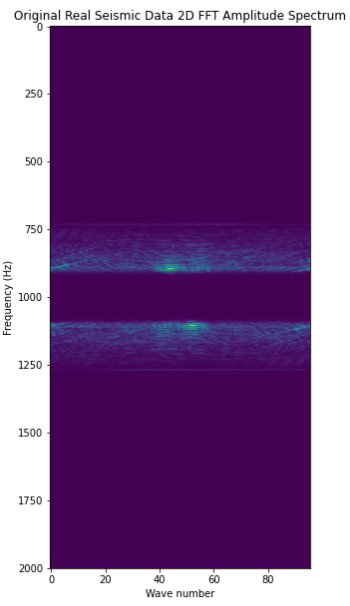
(a) Original Real Seismic Data



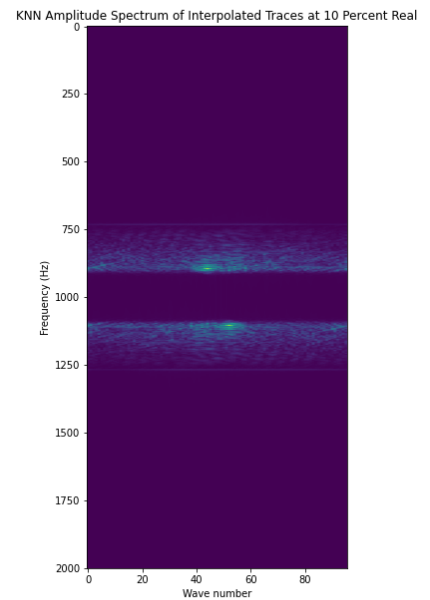
(b) Reconstructed Seismic Data After Interpolation



(c) Reconstruction Error

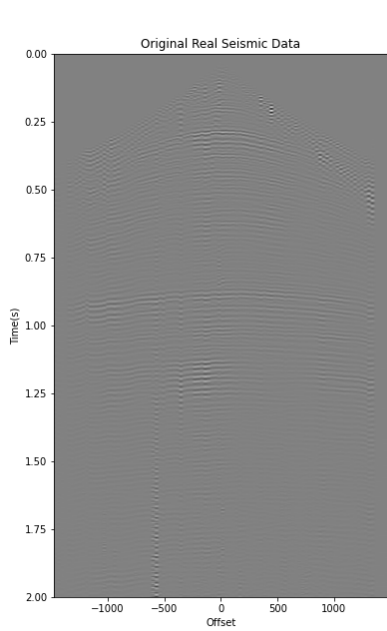


(d) Original Seismic Data 2D FFT

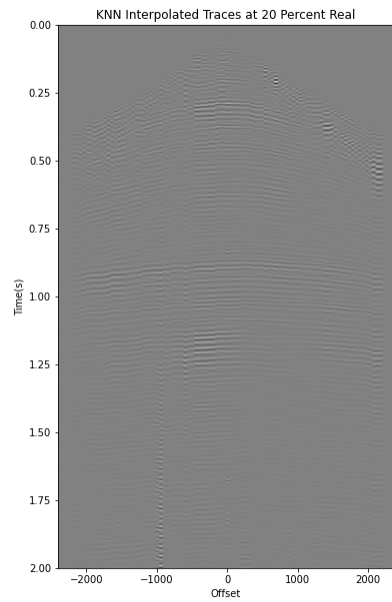


(e) Reconstructed Seismic Data 2D FFT

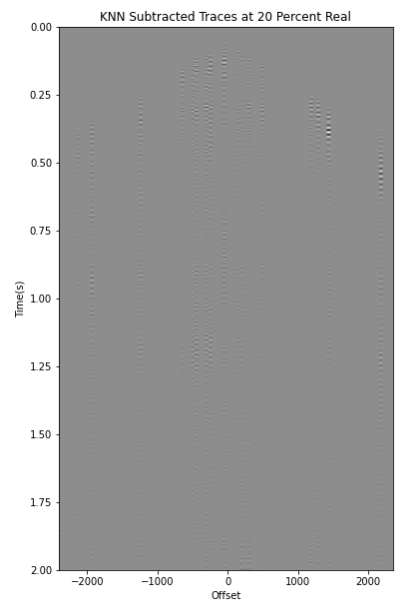
**Fig. 29:** KNN Result on Real Data at 10% Omitted Traces.



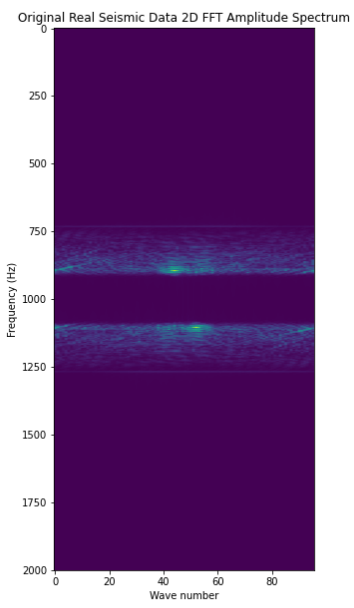
(a) Original Real Seismic Data



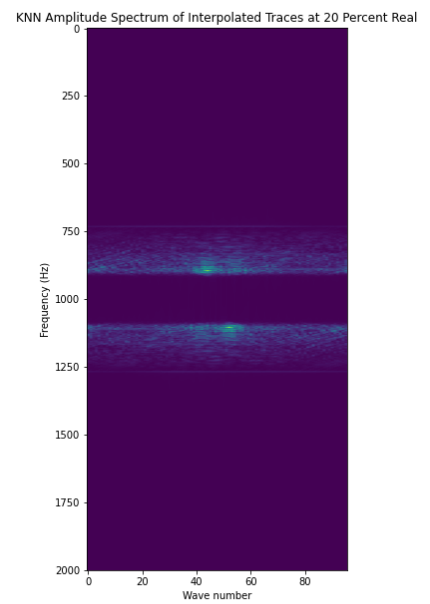
(b) Reconstructed Seismic Data After Interpolation



(c) Reconstruction Error

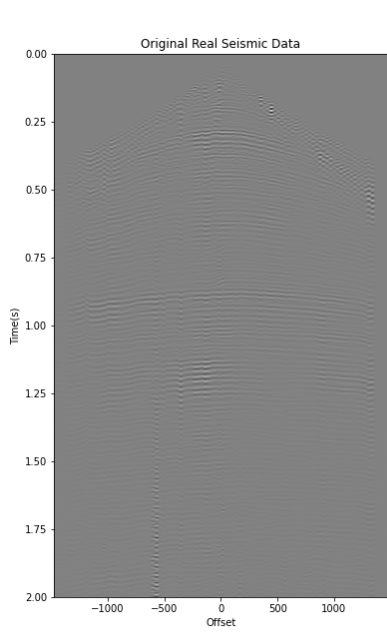


(d) Original Seismic Data 2D FFT

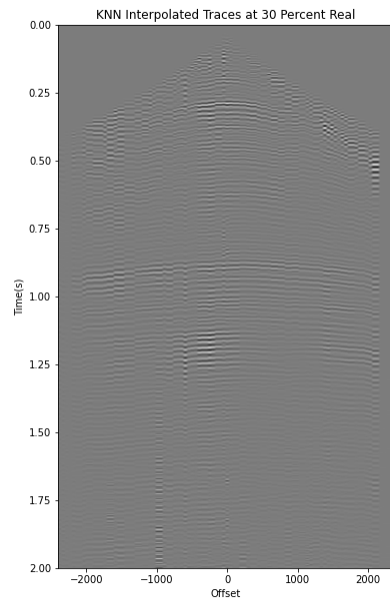


(e) Reconstructed Seismic Data 2D FFT

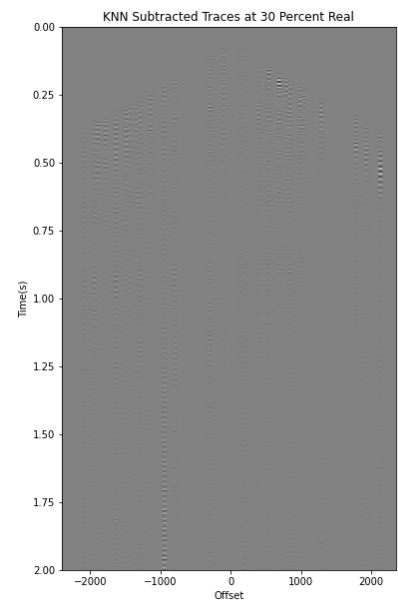
**Fig. 30:** KNN Result on Real Data at 20% Omitted Traces.



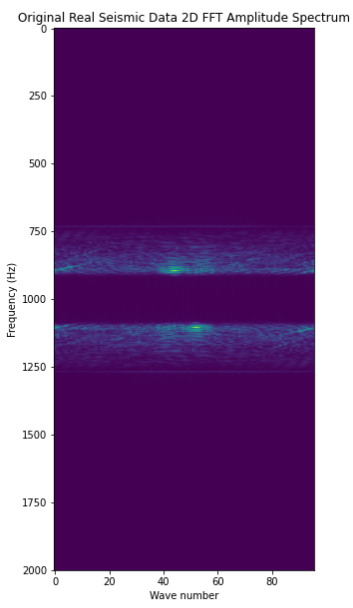
(a) Original Real Seismic Data



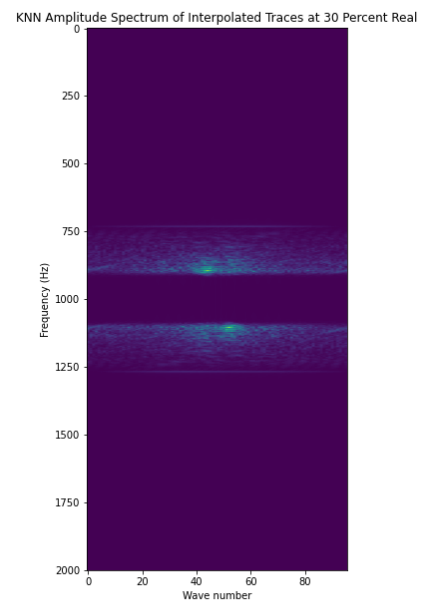
(b) Reconstructed Seismic Data After Interpolation



(c) Reconstruction Error

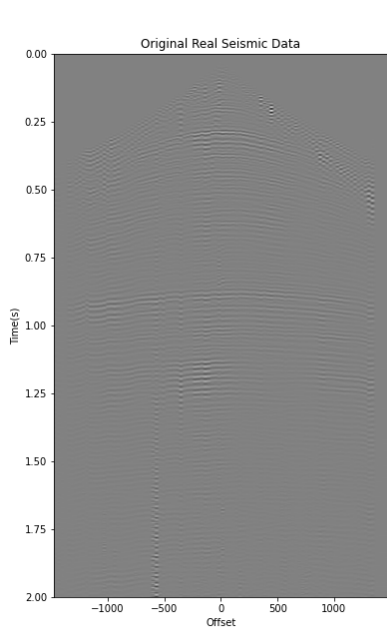


(d) Original Seismic Data 2D FFT

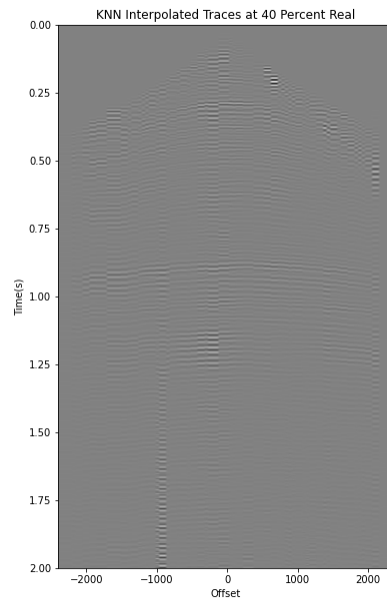


(e) Reconstructed Seismic Data 2D FFT

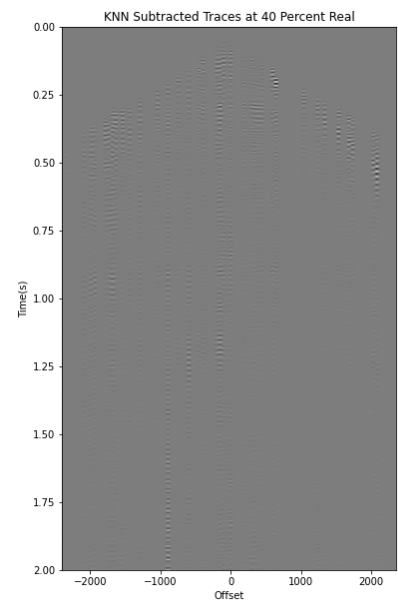
**Fig. 31:** KNN Result on Real Data at 30% Omitted Traces.



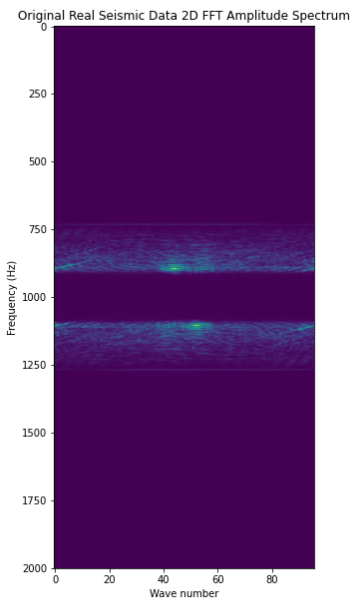
(a) Original Real Seismic Data



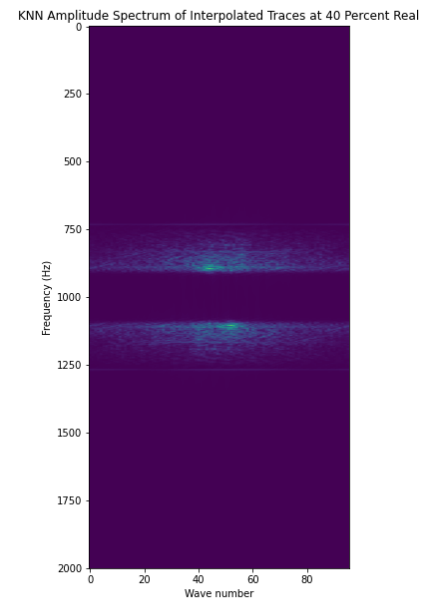
(b) Reconstructed Seismic Data After Interpolation



(c) Reconstruction Error

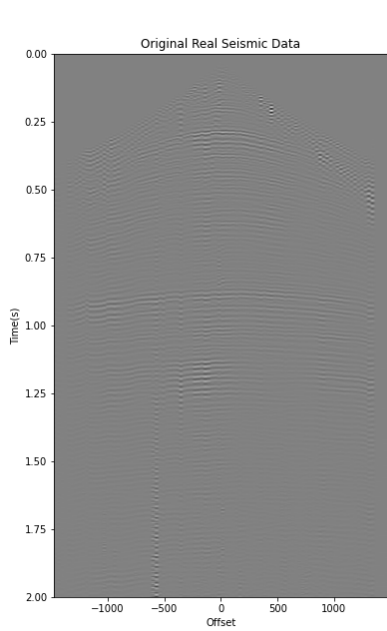


(d) Original Seismic Data 2D FFT

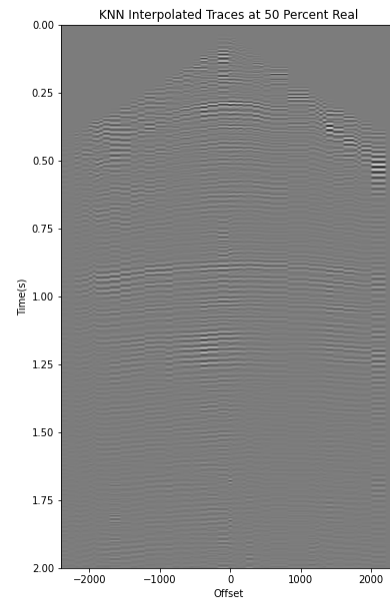


(e) Reconstructed Seismic Data 2D FFT

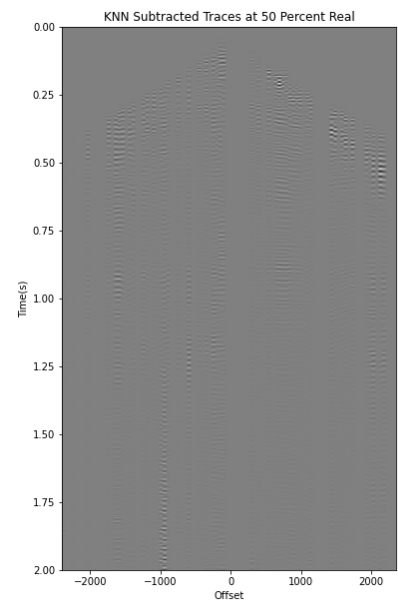
**Fig. 32:** KNN Result on Real Data at 40% Omitted Traces.



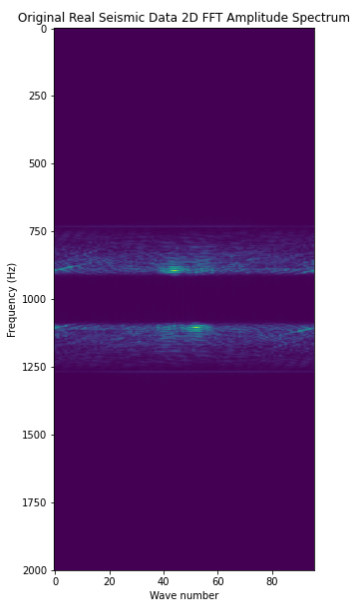
(a) Original Real Seismic Data



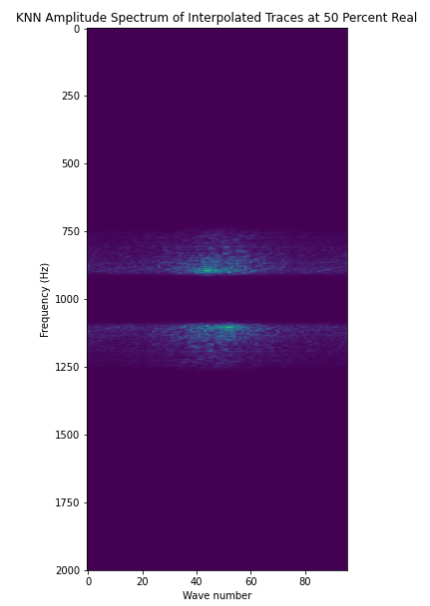
(b) Reconstructed Seismic Data After Interpolation



(c) Reconstruction Error

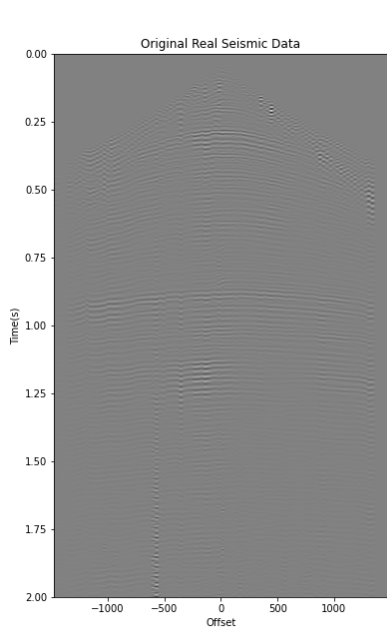


(d) Original Seismic Data 2D FFT

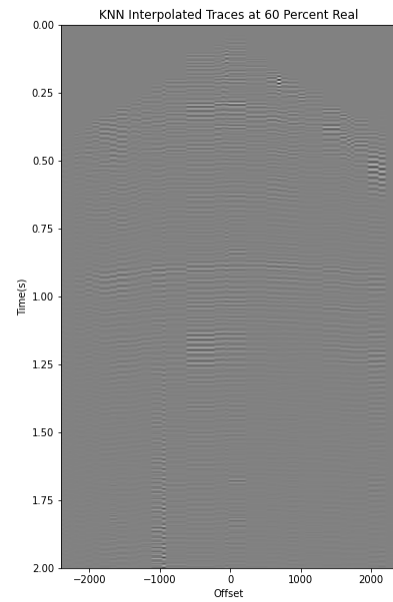


(e) Reconstructed Seismic Data 2D FFT

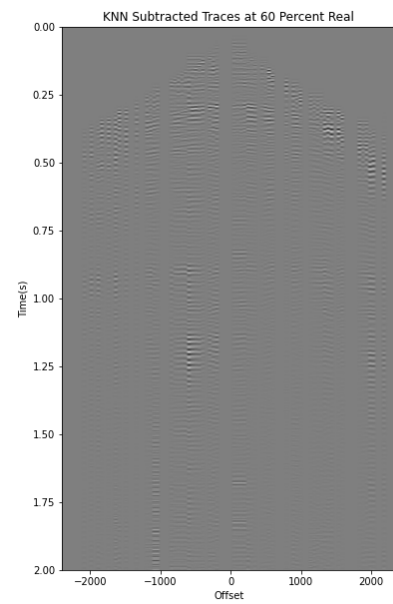
**Fig. 33:** KNN Result on Real Data at 50% Omitted Traces.



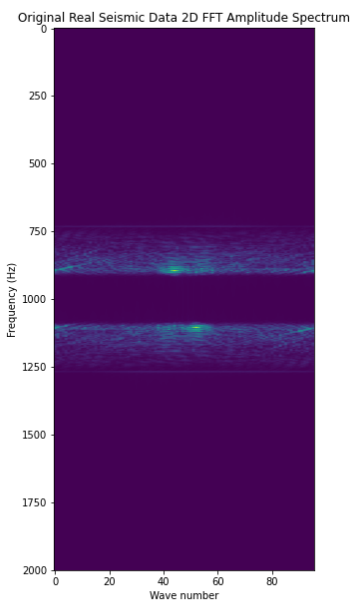
(a) Original Real Seismic Data



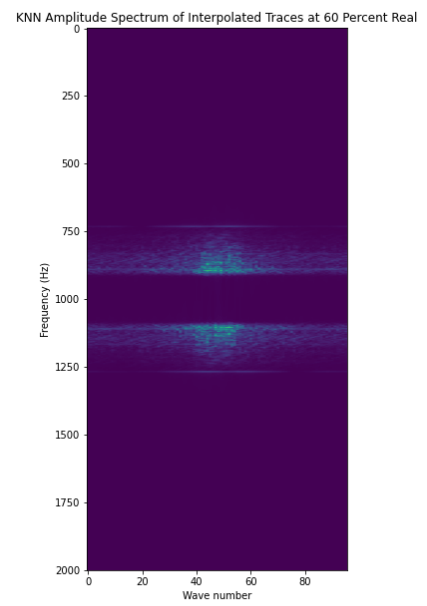
(b) Reconstructed Seismic Data After Interpolation



(c) Reconstruction Error

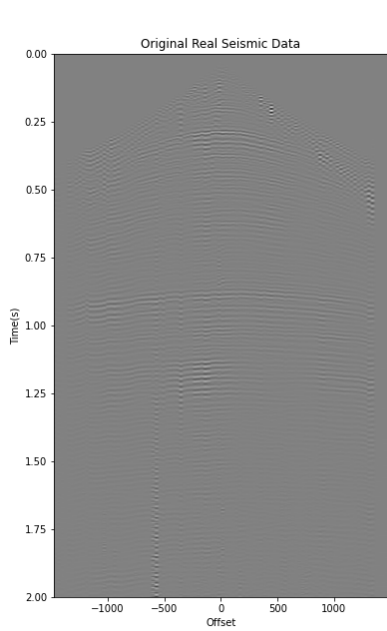


(d) Original Seismic Data 2D FFT

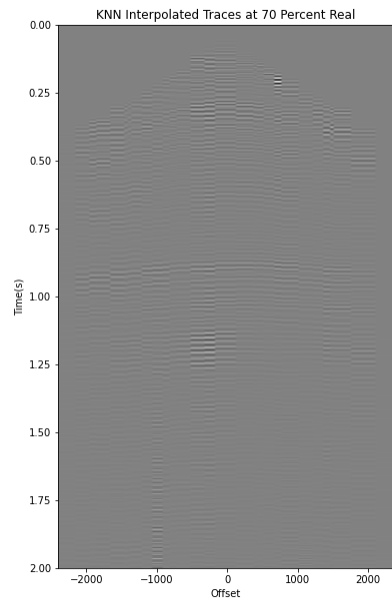


(e) Reconstructed Seismic Data 2D FFT

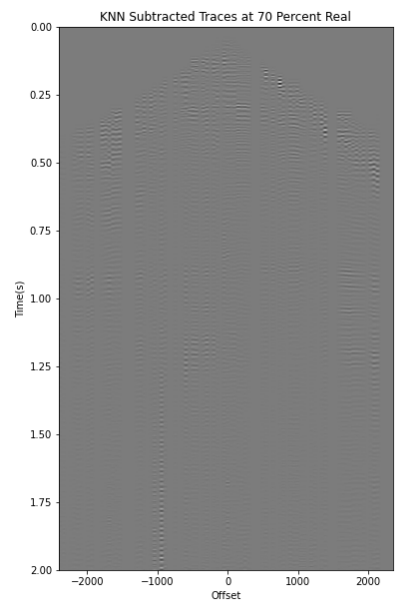
**Fig. 34:** KNN Result on Real Data at 60% Omitted Traces.



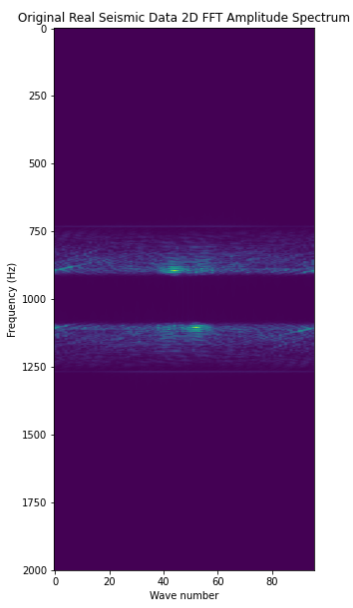
(a) Original Real Seismic Data



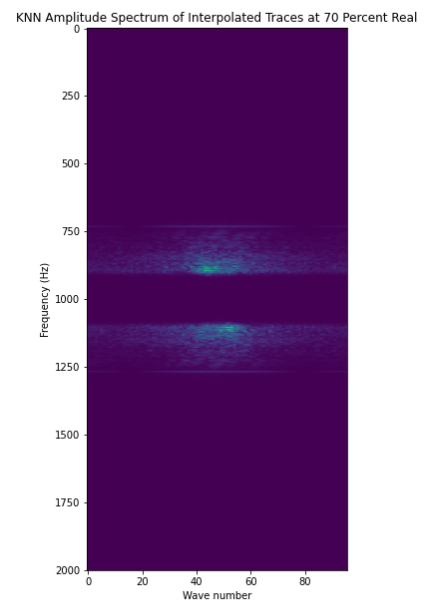
(b) Reconstructed Seismic Data After Interpolation



(c) Reconstruction Error

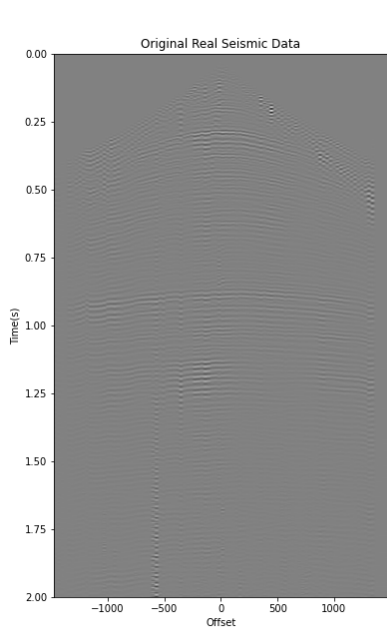


(d) Original Seismic Data 2D FFT

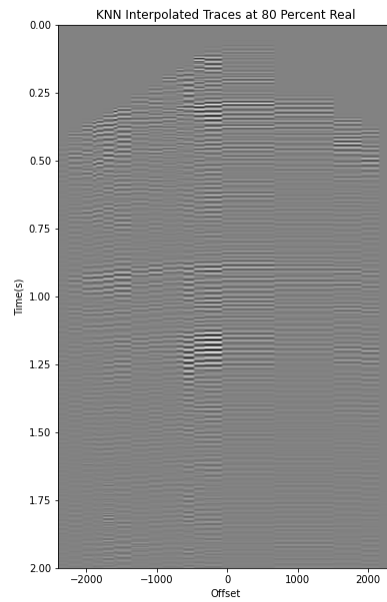


(e) Reconstructed Seismic Data 2D FFT

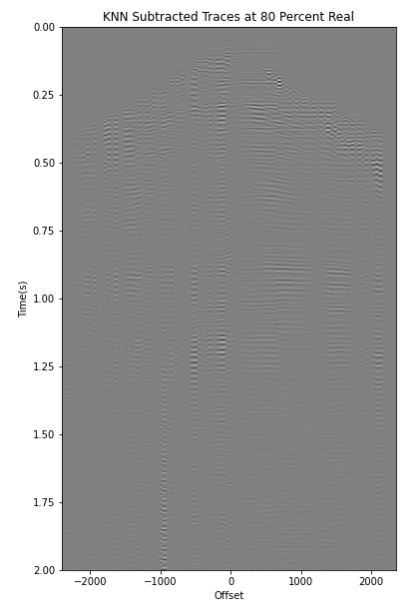
**Fig. 35:** KNN Result on Real Data at 70% Omitted Traces.



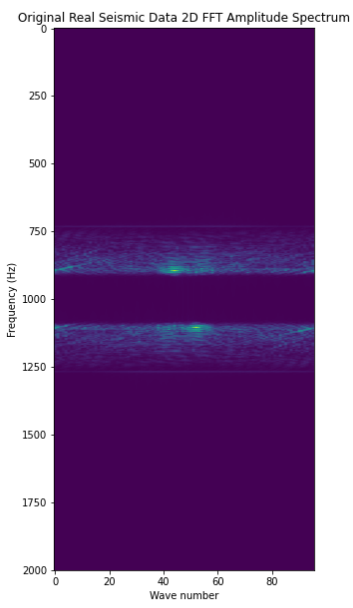
(a) Original Real Seismic Data



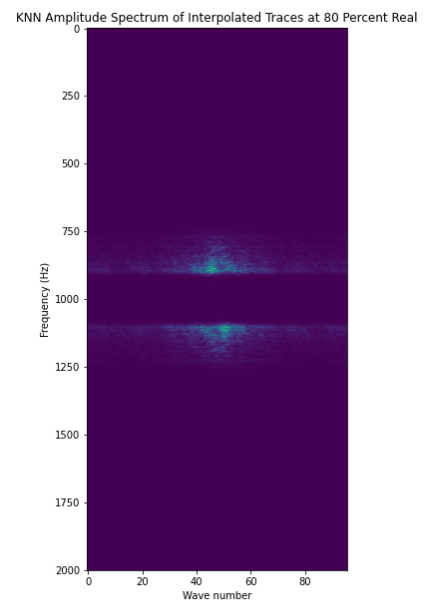
(b) Reconstructed Seismic Data After Interpolation



(c) Reconstruction Error

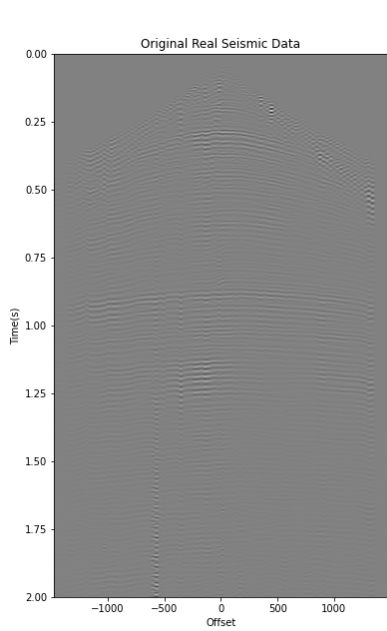


(d) Original Seismic Data 2D FFT

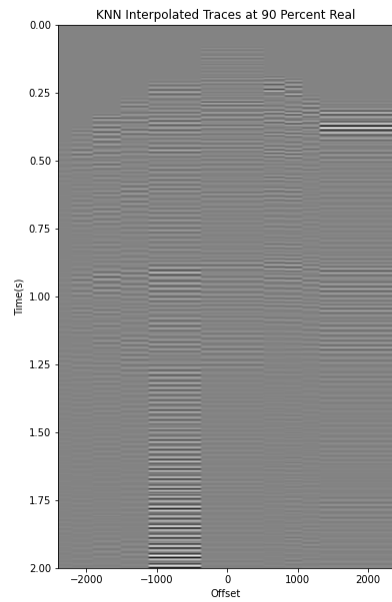


(e) Reconstructed Seismic Data 2D FFT

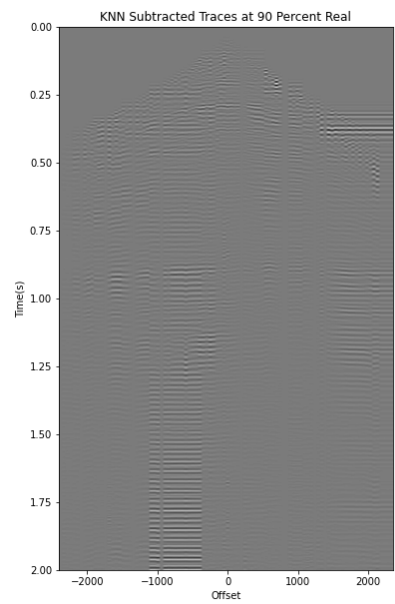
**Fig. 36:** KNN Result on Real Data at 80% Omitted Traces.



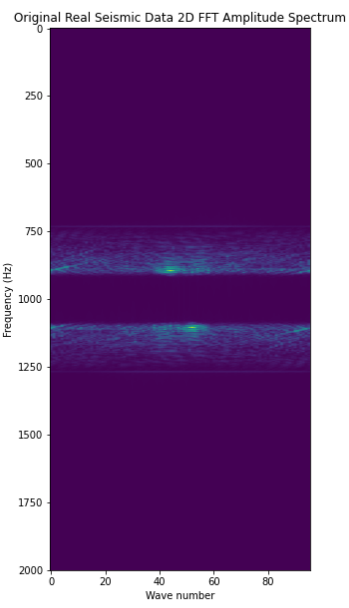
(a) Original Real Seismic Data



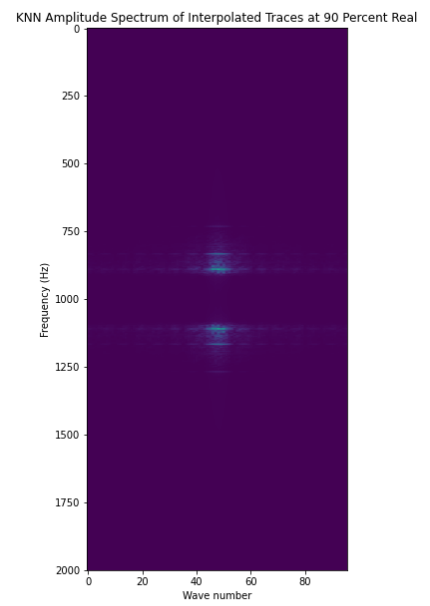
(b) Reconstructed Seismic Data After Interpolation



(c) Reconstruction Error

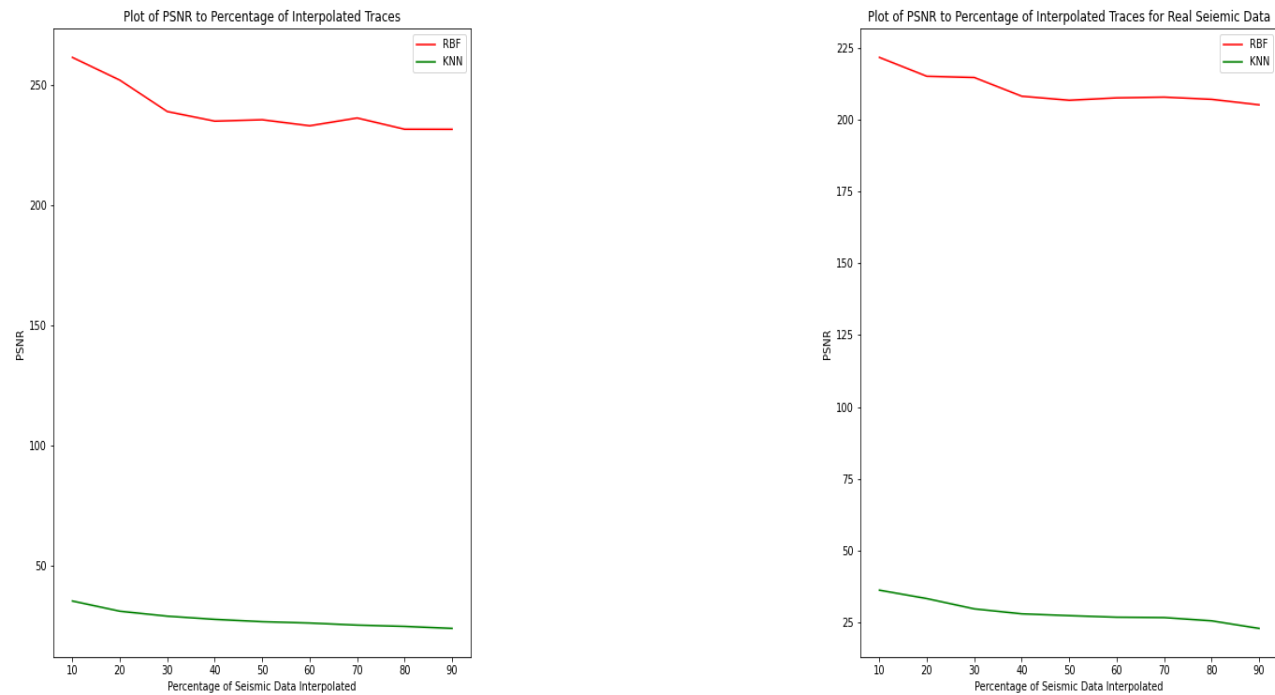


(d) Original Seismic Data 2D FFT



(e) Reconstructed Seismic Data 2D FFT

**Fig. 37:** KNN Result on Real Data at 90% Omitted Traces.



(a) Synthetic Seismic Data Interpolation PSNR for RBF and KNN

(b) Real Seismic Data Interpolation PSNR for RBF and KNN

**Fig. 38:** A plot showing PSNR of interpolated traces at different percentages for (a) Synthetic and (b) Real seismic shot gathers